



HAL
open science

A comprehensive review of biochar in removal of organic pollutants from wastewater: characterization, toxicity, activation/functionalization and influencing treatment factors

H. Zeghioud, Lydia Fryda, Hayet Djelal, Aymen Assadi, Abdoulaye Kane

► To cite this version:

H. Zeghioud, Lydia Fryda, Hayet Djelal, Aymen Assadi, Abdoulaye Kane. A comprehensive review of biochar in removal of organic pollutants from wastewater: characterization, toxicity, activation/functionalization and influencing treatment factors. *Journal of Water Process Engineering*, 2022, 47, pp.102801. 10.1016/j.jwpe.2022.102801 . hal-03655628

HAL Id: hal-03655628

<https://normandie-univ.hal.science/hal-03655628>

Submitted on 29 Apr 2022

HAL is a multi-disciplinary open access archive for the deposit and dissemination of scientific research documents, whether they are published or not. The documents may come from teaching and research institutions in France or abroad, or from public or private research centers.

L'archive ouverte pluridisciplinaire **HAL**, est destinée au dépôt et à la diffusion de documents scientifiques de niveau recherche, publiés ou non, émanant des établissements d'enseignement et de recherche français ou étrangers, des laboratoires publics ou privés.

23 the substrates' physiochemical properties, the role of the most used characterization
24 techniques toxicity, activation/functionalization and influencing treatment factors in
25 organic pollutant removal from wastewater.

26 The effect of different operating parameters of the water treatment process is summarized
27 and thoroughly discussed. The toxicity of biochar components such as heavy metals,
28 dioxins and polycyclic aromatic hydrocarbons (PAHs) is addressed. The various
29 application processes of biochar in water treatment at both laboratory and pilot scale is
30 also reviewed. The activation techniques, functionalization pathways and biochar based-
31 nanocomposite synthesis methods for enhancing the pollutant elimination efficiency are
32 also extensively discussed. Finally, the paper suggests research directions in the field of
33 biochar application in wastewater treatment.

34 **Keywords:** Biochar; Characterization; Toxicity; Contaminant removal; Functionalization;
35 Magnetization.

36

37 **1. Introduction**

38 The world population increase over the past two decades led to an increasing demand in
39 water volume, both for human consumption and for the industry sector, which results to
40 increased wastewater volumes released in the aquatic environment. A variety of pollutants
41 are detected in wastewater streams and have been reported in literature, such as;
42 carcinogenic heavy metals [1], petroleum hydrocarbons [2], polycyclic aromatic
43 hydrocarbons (PAHs) [3], organic dyes [4], phenols, pesticides, pharmaceuticals and
44 veterinary antibiotics [5]. A diversity of pollutant treatment techniques has been

45 extensively discussed in literature [6][7][8]. However, the design of optimal, efficient, and
46 operational treatment methods is still considered a challenge. Among different techniques
47 which have been the subject of research, we identified the most promising: chemical
48 oxidation, electrocoagulation, membrane separation, reverse osmosis, filtration,
49 adsorption and biological treatment [9][10][11].

50 Adsorption is one of the most efficient methods for the removal of a wide variety of
51 pollutants from gaseous and wastewater streams [12][7]. During the adsorption process
52 the pollutants are removed from the effluent by being adsorbed on the active sites on the
53 surface of a solid substrate (adsorbent). Certain parameters such as temperature, pH or
54 the concentration of adsorbate of the liquid phase influence the adsorption capacity and
55 their fluctuations can result to the desorption of the adsorbed species from the surface
56 back into the liquid phase [13].

57 Common adsorbents include clays, zeolites and active carbon, the latter being widely
58 used for efficient micropollutant removal especially in the potabilization of water.

59 Active carbon used in Europe is usually produced from biomass transported over long
60 distances, such as coco coir or coco shells, as well as coal. Local residual biomass and
61 well controlled pyrolysis conditions offer the advantage of sustainably produced
62 substrates, biochars, as an alternative to currently used active carbon [14].

63 The initial interest in biochar focused on the improvement of agricultural productivity via
64 enhancement of soil fertility, increasing soil nutrient levels and water retaining capacity,
65 while decreasing greenhouse gas emissions and carbon sequestration are drivers that
66 gain a lot of attention currently [15][16][17]. Biochar is considered a cost-effective and

67 environmentally friendly material [9][10], with large surface area, high porosity, functional
68 groups, high cation exchange capacity, stability, reusability [17][18]. These characteristics
69 make it a suitable substrate in environmental applications which have also gained a lot of
70 attention the last years. Some very recently published reviews demonstrate the effective
71 application of biochar for both heavy metals and organic pollutants (pesticides, phenols)
72 removal from contaminated soil [19][20][21]. Regarding the produced biochar properties,
73 these are related to the nature of the feedstock (lignocellulosic biomass: green waste,
74 organic residues, energy crops) and the preparation conditions.

75 Biochar is a high carbon containing material with high specific surface area and a large
76 porosity which is produced via the carbonization of biomass under a limited oxygen
77 environment [15]. The carbonization process allows the valorization of diverse biomass
78 sources like lignocellulosic residues from agro-industrial and forestry activities, animal
79 manure, dewatered sludges, even micro algae, marine and aquatic species [22][16].
80 Lignocellulosic biomass pyrolyzed at high temperature (>600°C) produces biochars with
81 high aromatic carbon content, high stability and therefore resistance to microbial
82 decomposition. Animal manure conversion produces biochar with high ash content and
83 therefore a very high pH value, due to the nutrients present in the feedstock. As a
84 consequence, biochar may act as a slow-release fertilizer and alkalinity regulator for acidic
85 soils. The high nutrients content of biochar is linked to its potential for soil cation exchange
86 capacity (CEC), water holding capacity and plays a role in the nitrogen cycle in soil.

87 The term carbonization includes the technologies of pyrolysis, hydrothermal
88 carbonization, flash carbonization, gasification and torrefaction [23][17][24]. These
89 technologies vary with respect to their relative co-products and their maximum yields

90 which are linked to the operating conditions such as pressure and temperature, its heating
91 rate and its residence time in the reactors [20][25]. Low carbonization temperatures
92 (<300–400 °C) result in low porosity biochars. Medium carbonization temperatures (400–
93 700 °C) yield biochars with the highest porous development and a higher aromaticity, the
94 latter promoting electron donor interaction [12]. At moderate pyrolysis temperature, the
95 biochar surface may contain oxygen and nitrogen surface groups, which add
96 functionalities and could act as electron acceptors. Biochar prepared at temperatures
97 above 700 °C are hydrophobic and recalcitrant, and have no apparent functionality
98 anymore due to the loss of almost all O and H in their structure [25].

99 The term functional biochar refers to biochars (a) either produced at low temperature and
100 thus still containing some O and H which allow the formation of surface functional groups,
101 but with the drawback of low porosity and surface area, or (b) produced at usual pyrolysis
102 conditions as presented earlier, and further treated either chemically or physically in order
103 to enhance its functional groups while keeping its high surface area porosity and
104 recalcitrance.

105 By further post treating biochars it is possible to obtain functional materials for
106 environmental applications, in water and air treatment of industrial effluents and off gases.
107 In specific, the application of biochar in wastewater treatment is believed to overcome the
108 problem of cytotoxic, genotoxic and mutagenic activities in living organisms resulting from
109 the application of ozonation, hydrogen peroxide, chlorine dioxide for organics pollutants
110 removal [26].

111 The adsorption efficiency of organic compounds on biochar is based mainly on
112 electrostatic interaction, partitioning, hydrophobic interaction, pore-filling, hydrogen

113 bonding formation, π - π interaction between biochar and organic pollutants [27].

114 The wide range of biomass feedstock used in the production of biochar in combination
115 with the production conditions applied, lead to a range of products with variable physico-
116 chemical composition and properties. There is a strong interest in linking biochar
117 physicochemical characteristics and their potential application.

118 Concerted efforts are being done to regulate and define quality requirements related to
119 biochar, develop guidelines for biochar and substrates used for its production. At this
120 moment, certain organizations are developing quality standards, namely the European
121 biochar certificates (EBC) in Europe, and the International Biochar Initiative (IBI) at
122 international level. The EBC indeed provides good suggestions to produce biochar that
123 can potentially be used in various applications but it is not their objective to make an
124 elaborate correlation between physicochemical characteristics and potential application.
125 This further elaboration of quality standards is the objective of ongoing research and
126 demonstration projects at EU level (ThreeC, HortiBlueC), to name a few.

127 Recent reviews aim to categorize the large amount of information of biochar
128 physicochemical properties and their effect on removal mechanisms by attributing
129 preparation technologies, functionalization techniques, to certain biochar characteristics
130 and propose specific applications, as for example in Wang et al and Patel et al.[28][29].

131 The knowledge of biochar characteristics and their possible effect on adsorption
132 mechanisms towards various types of pollutants in aqueous media is necessary to clarify
133 what steps to take towards improving biochar characteristics by means of various
134 treatments like activation and functionalization.

135 Table 1 gives a global overview of biochar properties, their function, their role in pollutant
 136 adsorption and relevant production parameter of biochar

137
 138 Table 1: Global overview of biochar properties, their function, their role in pollutant
 139 adsorption and relevant production parameter of biochar

Biochar Property	Function	Application/ mechanism involved	Biochar production parameter
SSA, porosity	sorption capacity	Immobilization of contamination from solid, liquid and gaseous media	Residence time, high temperatures
Ion-exchange properties on surface	electrostatic interactions with polar or non-polar groups	adsorption of organic contaminants	post functionalization (acidic or base treatment)
high mechanical and chemical stability			high temperatures
Surface functional groups	Chemical bonding with certain molecules	Absorption and immobilization of certain toxins and drugs	Low temperature production, post treatment (functionalization)
pH and pH_{pzc}	Negatively or positively charged surface	Attraction/repulsion of ionically charged molecules	Feedstock (high ash content biomass leads to high pH biochars), post functionalization (acidic or base treatment)

140
 141 This review aims to give the state of the art on the removal of toxic organic pollutants from
 142 wastewater using biochar, activated biochar, functionalized biochar and metal oxide or
 143 clay base biochar composites, commenting on the substrates' physicochemical
 144 characteristics, toxicity, activation/functionalization techniques and the link with the
 145 adsorption process parameters.

146 The impact of adsorption process parameters such as temperature, biochar loading,
 147 pollutants initial concentration, initial pH, presence of ions and contact time is discussed,
 148 to evaluate the activation/modification of biochars and their effect on the treatment

149 efficiency. This review paper also addresses recent biochar characterization techniques
150 giving information on the interpretation of analysis results mainly for FTIR, XPS, XRD,
151 TGA and Raman. The role of each technique on evaluating biochar properties is
152 underlined. Furthermore, the modification of certain biochar characteristics via activation,
153 functionalization and nanocomposite incorporation is discussed. The link between biochar
154 treatment/post-modification process and biochar properties is highlighted. This review
155 aims to contribute to the ongoing discussion and research efforts in EU and globally on
156 biochar quality standards, that may complement and elaborate the existing EBC and IBI
157 standards (European Biochar Certificate and International Biochar Initiative). This review
158 focuses on the applications of biochar in physicochemical treatments and does not
159 address biological processes that may include biochar at some stage.

160

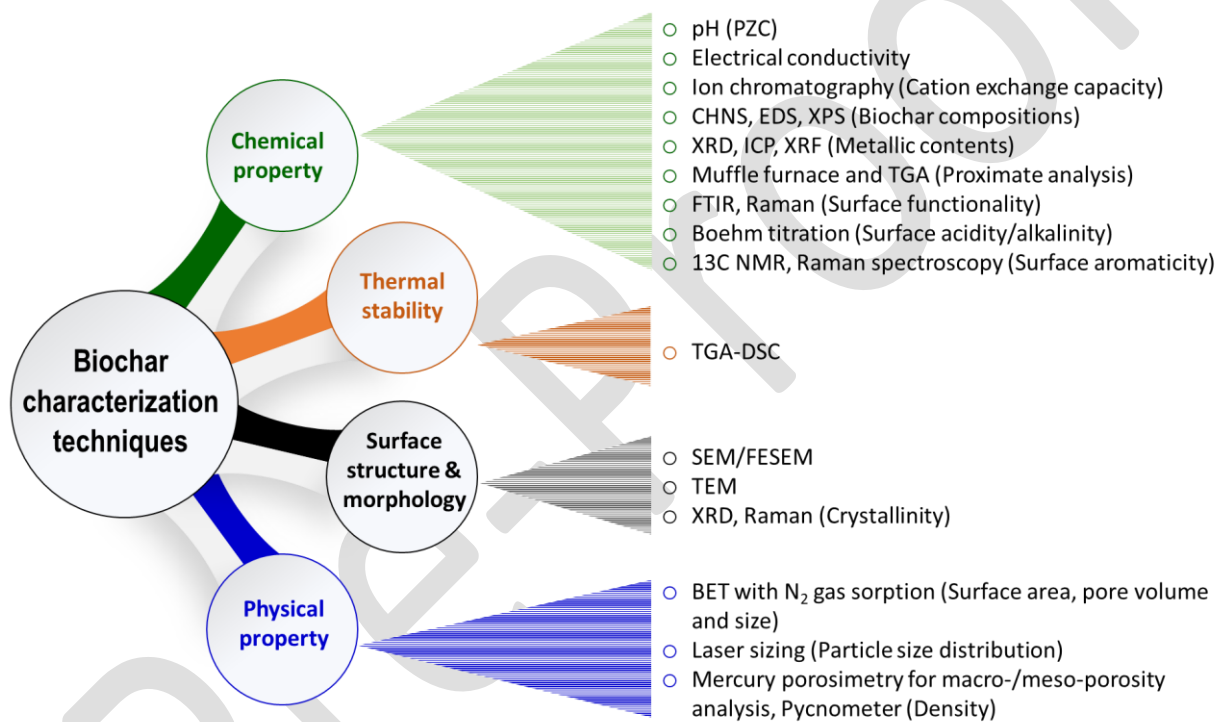
161 **2. Biochar characterization techniques**

162

163 Recent studies prove the importance of thorough biochar characterizations to help identify
164 agronomic and environmental applications and to distinguish biochar from other organic
165 matter that provide comparable functions, either as soil improver or environmental
166 applications [30][31]. The application area of biochar is large, depending on its
167 characteristics such as specific surface area, surface functional groups, stability and
168 structure and, to a lesser degree, elemental composition [32]. These characteristics make
169 the choice of appropriate characterization techniques for biochar of a great interest and a
170 difficult task at the same time. A judicious and complete characterization of biochar
171 preceding to any target applications requires a high level of understanding the correlations

172 between biochar production conditions and the physiochemical properties of the biochar
 173 [33][34]. The properties of biochar can be classified in four main categories: i) chemical
 174 properties (chemical composition, functional groups, pH, ion exchange capacity; ii)
 175 physical properties (porosity, pore size distribution, specific surface area); iii) structure
 176 and surface and morphology); iv) and thermal stability properties; each category requires
 177 specific characterization techniques as shown in figure 1.

178



179

180

181 **Figure 1:** Classification of characterization techniques versus biochar properties
 182 reported in biochar literature.

183

184 We would like to comment that the stability of biochar may be defined differently if one
 185 considers focusing on the evolution of physicochemical properties during applications as

186 a stability indicator. Stability of biochar in the soil for example, is evaluated in several ways
187 that include protocols of accelerated aging using chemical reagents, the objective of which
188 tests is to estimate the long-term carbon storage capacity of biochars in the carbon credit
189 context, or in GHG emission tests during incubation experiments to estimate the effect of
190 biochar/hydro char in compost. These applications deviate from the objective of this
191 review and will therefore not be further analyzed.

192 The characterization techniques reported in literature include Fourier Transform Infrared
193 Spectrometer (FTIR), Cation Exchange Capacity (CEC) [35], Scanning Electron
194 Microscopy (SEM), X-Ray Diffraction (XRD), X-Ray photoelectron spectrometry (XPS)
195 [36], Thermo Gravimetric Analysis (TGA), Differential scanning calorimetry (DSC),
196 Nuclear Magnetic Resonance (NMR), Raman spectroscopy, Brunauer Emmett Teller
197 (BET) [37].

198 Emerging pollutants appear in very low concentrations, in the range from $\text{ng}\cdot\text{L}^{-1}$ to $\mu\text{g}\cdot\text{L}^{-1}$,
199 so their elimination using conventional water treatment technologies is difficult. Only with
200 the development of novel analytical techniques or the further development of existing
201 ones, such as liquid chromatography coupled with mass spectrometry (LC-MS), can we
202 safeguard detection of micro pollutants. On the other side of the pollutant removal
203 challenge is the necessity for advanced solid materials characterization techniques, to
204 evaluate the effect of various production parameters and treatment techniques on biochar
205 and achieve therefore the necessary links among properties and applications, which is
206 much needed in standardization efforts of biochar quality. Research is advancing in the
207 development of both, accurate analytical techniques to quantify pollutants in very low
208 concentrations and in the development and characterization technologies for novel

209 functional biochar-based materials. These challenges go hand in hand and the effort to
210 categorize and standardize is a long and tedious task.

211 Biochar characterization techniques are crucial to evaluate the performance of novel
212 materials and to optimize the treatment process. Advances in characterization
213 technologies help in the direction of novel composites, however a review and deeper
214 analysis of characterization technologies is not in the scope of this article, beside
215 recommendations on the characterization technique chosen that will be commented upon.

216
217 Figure 2 shows the reporting frequency (%) of each characterization technique used in
218 biochar literature based on 100 scientific research articles (articles dated from 2018 to
219 2021). It seems that the surface imaging characterization techniques such as SEM and
220 TEM are the most applied with a frequency of 92/100, followed by specific surface area
221 quantification (BET) with 83/100, FTIR with 81/100 and then XRD, XPS and porosity with
222 63%, 55% and 47%, respectively. Nevertheless, the CEC, XRF and Boehm titration
223 remain the less used techniques applied to evaluate the physicochemical properties of
224 biochar. It can be concluded that surface morphology, crystallinity, the specific surface
225 area and surface functional groups are the most demanded properties and determining
226 factors in biochar engineering for organic pollutants removal. Concerning heavy metals
227 content quantification, Inductively Coupled Plasma (ICP) is much more broadly applied
228 than XRF.

229

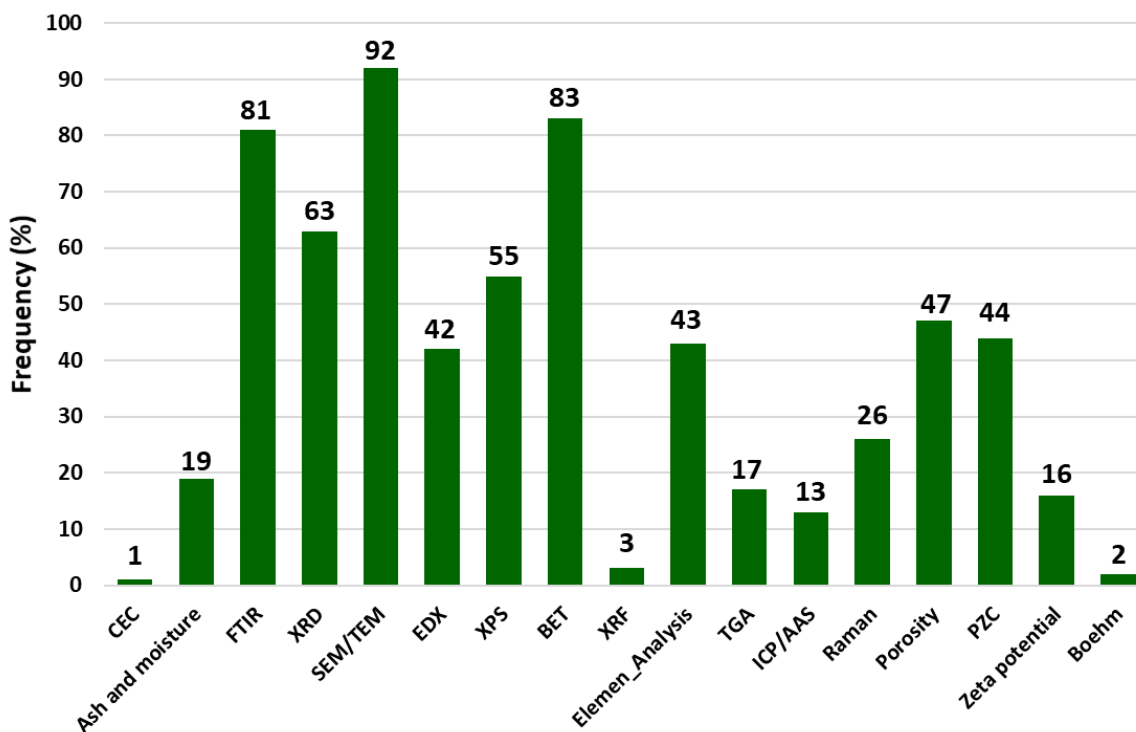


Figure 2: Frequency of applying certain techniques for biochar characterization (data recorded from 100 studies).

230
231
232
233
234
235
236
237
238
239
240
241
242
243

Table 2 shows a variety of functionalized novel biochar -based materials, with the potential to eliminate a variety of pollutants (antibiotics, dye, pesticides and steroids) at different treatment conditions. The categorization of table 2 is based on pollutant rather than biochar materials because at this stage of research it is not yet possible to discuss categories of novel functional materials and link “products” to pollutants to be removed. In the reported literature the efficiency of biochar in eliminating a pollutant is expressed both, as a removal efficiency (%) or as an adsorption capacity (mg/g). We observed that the acidic treatment is the most applied one for biochar modification/activation.

244 **Table 2:** Biochars applied in the treatment of organic pollutants.

Biochar material	Treatment of biochar	Pollutant (initial Concentration)	Removal yield or adsorption capacity (q _{max})	References
Medicine (antibiotics)				
Cobalt-gadolinium modified biochar		Ciprofloxacin (20 mg/L) Tetracycline (20 mg/L)	99.55% (6 h) 99.23% (6 h)	[38]
Sulfamic acid modified biochar		Tetracycline (100 mg/L)	412.95 mg/g biochar	[39]
Activated biochar derived from cotton shell		Sulfadiazine (10 mg/L)	≈95% (1400 min)	[36]
Rice husk Carbonization at 500 °C	H ₂ SO ₄ or KOH treatments activation biochar	Tetracycline (20 mg/L)	93.1% (180 min)	[40]
Rice straw and swine manure Carbonization at 700 °C	H ₃ PO ₄ modified biochar	Tetracycline (C ₀ = 30–200 mg·L ⁻¹)	T = 25 °C pH = 5.0–9.0 q _{max} = 167.5 mg·g ⁻¹	[41]
Iron oxide nanoparticle loaded biochar		Ofloxacin (30 mg/L)	96% (5 h)	[42]
Bamboo Carbonization at 380 °C	H ₃ PO ₄ treatment	Sulfamethoxazole, sulfathiazole and sulfamethazine	T = 21–30 °C pH = 1.0–10.0 q _{max} SMX = 88.1 mg·g ⁻¹ q _{max} STZ = 237 mg·g ⁻¹ q _{max} SMZ = 65.7 mg·g ⁻¹	[43]
Anthriscus sylvestris-derived activated biochar	NaOH treatment	Diclofenac (DF) Cephalexin (CPX)	q _{max} = 392.94 mg g ⁻¹ for DF q _{max} = 724.54 mg g ⁻¹ for CPX	[44]
Dyes				
CaWO ₄ -biochar nanocomposites		Rhodamine (0.01 mM) Methyl orange (0.05 mM)	71% (30 min) 73% (30 min)	[45]
ZnO/biochar nanocomposites		Methylene blue (160 mg/L)	95.19% (225 min)	[46]
Fe, N codoped biochar		Acid orange (20 mg/L)	93.4% (20 min)	[47]
Pinecone biochar		Black-3	346.856 mg g ⁻¹	[48]
Pesticides				
P doped biochar		Triazine (2 mg/L)	>96% (20 min)	[49]

Sawdust-coal biochar		Epoxiconazole (10 mg/L)	97 % (400 min)	[50]
Grape pomace-derived biochar		Cymoxanil pesticide (100 mg/L)	q _{max} =161 mg /g biochar	[51]
CO ₂ activated biochar		Phenol (0.5 mM) Chlorophenol (0.5 mM)	50 – 60% (60 min)	[52]
Activated magnetic loofah sponge biochar	KOH treatment	Imidacloprid	q _{max} =738 mg.g ⁻¹	[53]
Steroides				
Graphene oxide supported on activated magnetic biochar		17 β -estradiol (6 mg/L)	q _{max} =46.22 mg/g biochar	[54]
Iron loaded porous graphitized biochar		17b-estradiol (3 mg/L)	100 % (45 min)	[55]

245

246

247 2.1. Physical proprieties.

248

249 Physical properties include the specific surface area (SSA), particle size distribution, the
 250 bulk density, pore size and pore volume distribution [55]. These parameters are directly
 251 linked to the biochar production conditions such as reactor temperature and residence
 252 time, addition of oxygen containing media in the process (air, pure oxygen, CO₂ and
 253 steam) and/or post production processing to modify the product [38]. In the work of Xiong
 254 et al., five different biochars from various feedstocks were applied on the adsorption of
 255 epoxiconazole (EPC) fungicide. The results showed that the adsorption capacity of these
 256 five biochars towards EPC is closely related to the total pore volume and specific surface
 257 area [50]. Patel et al. also reported a positive correlation between the biochar sorptive
 258 potential toward ciprofloxacin/acetaminophen, the biochar surface area, and the total pore
 259 volume [33].

260 Beside total surface area also biochar surface heterogeneity plays an important role in the
261 sorption behavior. The BET analysis is applied to study the effect of biochar modification
262 on SSA as discussed in Figure 5 or to evaluate the effect of pyrolysis temperature on SSA
263 of produced biochar. In their work Liu et al. reported the increase of SSA and total pore
264 volume with increasing pyrolysis temperature. In the presence of acid the accumulation
265 of inorganic content and the formation of new minerals at the biochar surface further
266 increased the SSA [39]. In addition to an increase in total pore volume, Cai et al. reported
267 a reduction in pore size [56].

268

269 **2.2. Chemical properties.**

270

271 Chemical properties of biochar include the point of zero charge (PZC), Cation Exchange
272 Capacity (CEC), surface functional groups and electrical conductivity. The structural and
273 elemental analysis are important to predict the impact of biochar on the environment [57].

274 The SEM technique is coupled with energy-dispersive X-ray spectroscopy (EDX or EDS)
275 to obtain insight to the O/C atomic ratio, elemental components composition and
276 distribution at the surface, and further on to explain the relationship between biochar
277 preparation parameters and its resulting properties. For example, the O/C atomic ratio
278 reflects the carbonization degree of the biochar, and indicates the degree of aromaticity
279 of biochars, which is linked to their stability and therefore to its carbon sequestration
280 potential [58].

281 On the other hand, EDX is reported as a potential tool for the direct O/C atomic ratio
282 measurement rather than applying the CHNS elemental measurement [58][59]. Some

283 works reported that the H/C and O/C atomic ratios in biochar have a positive correlation
284 with the concentration of hydroxyl, carboxyl, and carbonyl groups and thereby to CEC
285 [60][61]. The elemental ratios of H/C refer to the aromatization degree of carbonization
286 [62]. However, the value of O/C also represents the hydrophilicity of biochar [63].

287 XPS analysis is a very valuable characterization technique to identify the components
288 functional groups on the biochar surface and their metallic state of compounds, before
289 and after biochar composite synthesis [64]. XPS spectral lines (C 1s, O 1s and N 1s
290 photoelectron lines) are rich in chemical information (Table 3). Their precise positions on
291 the energy axis reflect the local electronic environment of the photoemitting atom, a clear
292 shift for C-O, C = O, COO⁻ and CO₃²⁻ carbons can be seen [65]. Zhang et al confirmed
293 the presence of Fe-O in biochar/Fe_xO_y composite by XPS at binding energies of 711.3
294 and 725.0 eV for the Fe 2p_{3/2} and Fe 2p_{1/2} core levels, respectively. Moreover, the
295 adsorption of methylene blue leads to a decrease in peaks intensities for the majority of
296 C 1s and O 1s spectrum [66]. On the other hand, the appearance of N 1s in the XPS
297 spectrum of biochar/Fe_xO_y-MB suggested that the adsorption involves N electrostatic
298 attraction [66][67]. The incorporation of Mn on Nano-zerovalent manganese/biochar
299 composite resulted to the detection of Mn²⁺ and Mn³⁺ present at binding energy values of
300 642.5 eV (Mn 2p_{3/2}), 653.5 eV (Mn 2p_{1/2}) for Mn²⁺ and 645.3 eV that corresponds to
301 Mn³⁺ [68]. Other works reported the presence of; i) O-Fe (530.12–530.26 eV) in O1 s XPS
302 spectra of biochar/Fe composites [69]; ii) Fe2p and Co2p at 711.3 eV and 779.8 eV,
303 respectively [70]; iii) Cr³⁺ at 584.20 and 575.04 eV [71].

304

305 **Table 3:** Binding energy in XPS spectra for the main surface functional groups on biochars
 306 reported in literature.

Biochar	C 1s Line					O 1s Line		N 1s Line	Reference
	C-C	C = C	C-O	O-C-O	C=O	Organic C=O	Organic C-O	C-N	
Biochar/Fe _x O _y composite	284.8	284.8	286.1	288.3		533.3	531.62	399.6 and 402.0	[66]
Biochar	284.4–284.7 285.0–285.2		286.3 – 286.6	289.1–289.3	287.8–288.0	531.3–532.3	533.3–533.9	399–401	[65]
Biochar/Fe composites						531.44–531.57	532.23–533.08		[69]
Graphene oxide /CoFe ₂ O ₄ sludge biochar composite	284.8	284.8	286.5						[70]
Iron-loaded biochar	284.8	284.8						400.2	[71]
Biochar-based iron oxide	284.4		285.6		288.5				[72]

Sludge-derived biochar			285.9 – 286.4	288.7– 289.0	287.1– 287.2				[73]
N-doped graphite-like mesoporous structure biochar			285.0 286.4		288.8			398.4, 400.0, 400.9	[74]
Magnetic sludge biochar	284.8	284.8	286.5		288.7				[75]
Ga ₂ S ₃ /S-modified biochar	285.62 283.77	285.6 2 283.7 7	284.0 3 285.3 4			532.27, 531.71, and 530.32			[76]
Hickory chip biochars	284.8	284.8	286		288.5	531.5	533.0		[77]

307

308 XPS can also be used to evaluate the elemental O/C molar ratio that may be considered

309 as an indication for biochar stability [78].

310 The use of Fourier Transform Infrared spectroscopy (FTIR) in biochar surface

311 characterization is also very common. This technique gives detailed information on the

312 oxygen-containing functional groups present on the surface of biochar (Table 4),

313 evaluates the success of metal binding during surface treatment and/or the surface

314 functional groups transformation after pollutants adsorption [54]. Al-Wabel et al reported

315 the increase of the broad absorption band attributed to O–H stretching vibrations (at

316 around 3320 cm^{-1}) in biochar with the moisture increase, however the presence of C–O–
 317 C stretching vibrations band indicated the occurrence of non-decomposed oxygenated
 318 groups [79]. FTIR can analyze organic functional groups commonly observed in biochars,
 319 as carbon-hydrogen (C-H), C = C, C=O, C-O, and silicon-oxygen (Si-O)[80][81]. Table 4
 320 shows the functional groups and their wavenumber in published literature on biochar and
 321 biochar composites.

322
 323 **Table 4:** Peak positions of the main surface functions in FTIR spectra of biochar and
 324 biochar-based composites reported in literature.

Biochar	O–H	C–O– C	C = C	Carboxyl C=O	C-O	C–H aromatic	C-N	Reference
Biochar/ Fe_xO_y composite	3368- 3429		1620	1386	1049	826		[66]
Alkali-modified SCG biochars	3160- 3430	1150- 1050		1600 – 1450				[82]
Nano-zerovalent manganese/biochar	3320		1580					[68]
Graphene oxide / CoFe_2O_4 sludge biochar composite	3423– 3444		1562– 1628		1035– 1081			[70]
Biochar derived from sugarcane bagasse	3430		1625	1710	1030	865– 750		[83]

Biochar-supported MnFe ₂ O ₄	3361		1495 and 1283			875		[84]
Bidirectional activated biochar from sugarcane	3744		1615, 1580, 1582, 1497		1415 and 1381		1384, 1379	[85]
Biochar-based iron oxide	3400–3500		1500	1600	1040			[72]
Sludge-derived biochar	3420	1035		1590	1035	700–900		[73]
Natural iron ore – biochar	3426		1588		1099	807		[86]
Pyrrolic N-rich biochar	3428		1592	1714	1064		1236	[56]
N-doped graphite-like mesoporous structure biochar	3160			1683–1590			1344	[74]
Magnetic Pristine biochar	3451		1584		1118			[87]
Biochar from oil palm frond	3460		1615	1736		878, 809 and 764		[88]
Biochars produced from rice straw, bagasse, and eucalyptus wood	3400		1620	1730	1100			[89]

Cornstalk, orange peel, and peanut hull derived biochar	3430		1620	1580	1080			[90]
Biochars from forest and agri-food wastes	3440		1633			877		[91]
Modified magnetic biochar from pine nut shells	3360	1030	1640				1050	[92]
Magnetic sludge biochar	3429– 3432	1031– 1090	1618– 1649					[75]
Cassava ethanol sludge derived biochar	3425– 3433	1066– 1087		1633– 1635				[93]

325

326 **2.3. Surface structure and morphology**

327

328 The surface morphology and chemical composition are important attributes of biochar.

329 Scanning electron microscope (SEM) and transmission electron microscope (TEM) are

330 valuable tools to evaluate the development of surface structure, porosity and pores

331 distribution of biochar before and after modification [38].

332 Raman spectroscopy is considered a powerful technique for exploring the graphitization

333 or defects on carbonaceous materials. In biochar engineering and development, the

334 interest focuses on two bands; i) the D band which represents the disorder and defect

335 degree caused by vacancies, edges and functional groups, ii) the G band which is related

336 to the crystalline and graphitic structures [94]. Meanwhile, the estimated intensity ratio of
 337 the D band relative to the G band (ID/IG) reflects the disorder and level of defect of the
 338 analyzed biochar (Table 5). It is suggested that an increase in ID/IG ratio due to the
 339 addition of iron suggests an increase of defective sites [95]. It is also reported that the
 340 increase in pyrolysis temperature until a certain value increases the defected sites formed
 341 on biochar [73]. Also a low ID/IG ratio meant a relatively high degree of graphitization [93].
 342 Generally, the ID/IG value increases with increasing pyrolysis temperatures, indicating
 343 that high pyrolysis temperatures are beneficial for the growth of defect structures in
 344 produced biochar [96][97].

345
 346 **Table 5:** The position of D band and G band in Raman spectra of biochar reported in
 347 literature.

Biochar	D band position (cm ⁻¹)	G band position (cm ⁻¹)	ID/IG	Reference
Sludge-derived biochar	1350	1580	0.84 and 1.06	[73]
Magnetic biochar derived from banana peels	1338	1589	0.94 and 0.99	[95]
Pyrrolic N-rich biochar	1343	1588	0.79 and 1.07	[56]

Multi-porous biochar from lotus biomass	1340	1585	1.67, 1.48, 1.30, and 1.56	[98]
Cassava ethanol sludge derived biochar	1368	1594	0.389 and 0.407	[93]
Graphitic biochar	1310	1590	1.94–2.56	[99]
Nanoscale zero-valent iron (nZVI) supported on rice stalk (RS) derived biochar composite	1309.1 1349.6	1561.7 1590.6	0.99, 1.04, 1.08, 1.05 and 1.10	[97]

348

349 The X-Ray Diffraction (XRD) technique is applied to determine the crystal structures and
350 phase composition in a solid material. It can also evaluate the ratio of crystalline and
351 amorphous phase and define the material modification such as metal oxide loading [64],
352 magnetic biochar composite synthesis [70]. The technique can evaluate the stability of
353 biochar components after modifications, for example SiO₂ modification [66]. The use of
354 XRD spectra is reported to evaluate the interlayer spacing of the activated biochar
355 according to Bragg's formula and/or the average crystalline size with the help of the
356 Scherrer equation [83].

357 **Bragg's equation:**

358

$$d = \frac{\lambda}{2\sin\theta}$$

359 In which λ is the X-ray wavelength whose value is 0.154 nm generally, and θ is the angle
360 of the peak position.

361 **Scherrer equation**

362 This equation is used to evaluate the average crystalline size along c-axis (L_c) and the
363 size of the layer planes (L_a).

364

$$L = \frac{k\lambda}{B\cos\theta}$$

365 In which k is the value of the shape factor ($k = 0.9$ and 1.84) which are used frequently for
366 the purpose of calculation of L_c and L_a respectively. B is the value of line broadening at
367 half width of the peak known as FWHM (Full width half maximum) in radians.

368

369 **2.4. Biochar stability**

370

371 Thermogravimetry analysis (TGA) is applied to evaluate the thermal stability of biochar
372 [74] and characterize its structure, as it gives information about the pyrolysis yield, the
373 content of moisture and the different structural components such as hemicellulose,
374 cellulose, and lignin [100]. Generally, the weight loss in TG analysis can be divided into
375 three stages shown in Table 6 below; the first stage represents the loss due the water
376 evaporation, and decomposition of bonded hydrated compounds, during the second stage
377 the major loss observed is explained by the thermal decomposition of polar organic
378 compounds derived from most cellulose, hemicellulose and holocellulosic precursors

379 [101]. Finally the last weight loss stage was attributed to the slow and gradual thermal
 380 decomposition of high molecular weight components present in the biomass [89].

381
 382 **Table 6:** The main weight loss stages of biochars in thermogravimetry analysis reported
 383 in literature.

Biochar	1st weight loss	2nd weight loss	3rd weight loss	Reference
Biochars produced from rice straw, bagasse, and eucalyptus wood	7 to 9 % (0-150 °C)	60 to 81 % (200-450 °C)	(450-900 °C)	[89]
Maple leaf-derived biochars	10 % (40-300 °C)	45 % (300-400 °C)	5 % (400-1000 °C)	[101]
Multi-porous biochar from lotus biomass	10 % (0-160 °C)	58 % (160-365 °C) dehydration and condensation of cellulose and hemicelluloses	20 % (350-900 °C)	[98]
Functionalized magnetic biochar from waste poplar sawdust (CoFe ₂ O ₄ @PBC-LDH)	11 % (20-200 °C) loss of hygroscopic water and light components	12-14 % (200-415 °C) dehydroxylation of LDHs and the release of volatile substances by the	17 % (415-980 °C) decomposition of biochar	[102]

		interlayer CO_3^{2-} anions		
--	--	---	--	--

384

385 **3. Toxicity of biochar**

386

387 Biochar has an active role in environmental remediation as an adsorbent, filter medium or
 388 active catalytic composite [103], nonetheless it is imperative to systematically discuss its
 389 potentially negative environmental effects and prevent risks during application. Some
 390 studies focus on the evaluation of harmful components of biochar such as dioxins [104],
 391 heavy metals [105], polycyclic aromatic hydrocarbons (PAHs) [106][107], environmentally
 392 persistent free radicals (EPFRs) [108], volatile organic compounds (VOCs) and
 393 perfluorochemicals (PFCs) [109].

394 The content of heavy metals in biochar differs with biomass type and source [105][110],
 395 for example sludge biochar, which has a high heavy metal content [111]. The
 396 concentration of heavy metals in biochar is therefore linked to the origin biomass and is
 397 retained during pyrolysis [112]. In addition, PAHs in biochar are reported to have high
 398 biotoxicity effect on plants and microorganisms in different environmental media. The
 399 content of PAHs in biochar depends on the process itself, namely residence time,
 400 temperature and special attention should be given to avoiding the condensation of tar
 401 loaded gases on the biochar. In specific, PAH formation i) varies with the feedstock type
 402 or nature [57], ii) is reduced at sufficient heating rate during pyrolysis [107], iii) decreases
 403 while pyrolysis temperature and/or residence time in reactor increase [113].

404 Dioxins also form during the biochar production process, the factors that influence are; i)
 405 Chloride (Cl) content in feedstock, as reported by Wiedner et al. [114], ii) reactor

406 temperature, with dioxins forming as temperature reduces, usually when the flue gas cools
407 down [107]. EPFRs can be produced during pyrolysis process with lignin, cellulose and
408 hemicellulose in biomass fibers acting as a precursor [115], [116]. In addition, the content
409 of these free radicals increases with the pyrolysis temperature [117]. It may pose a
410 potential environmental risk since they can induce the formation of reactive oxygen
411 species with high cytotoxicity and phytotoxicity within environmental media [118].

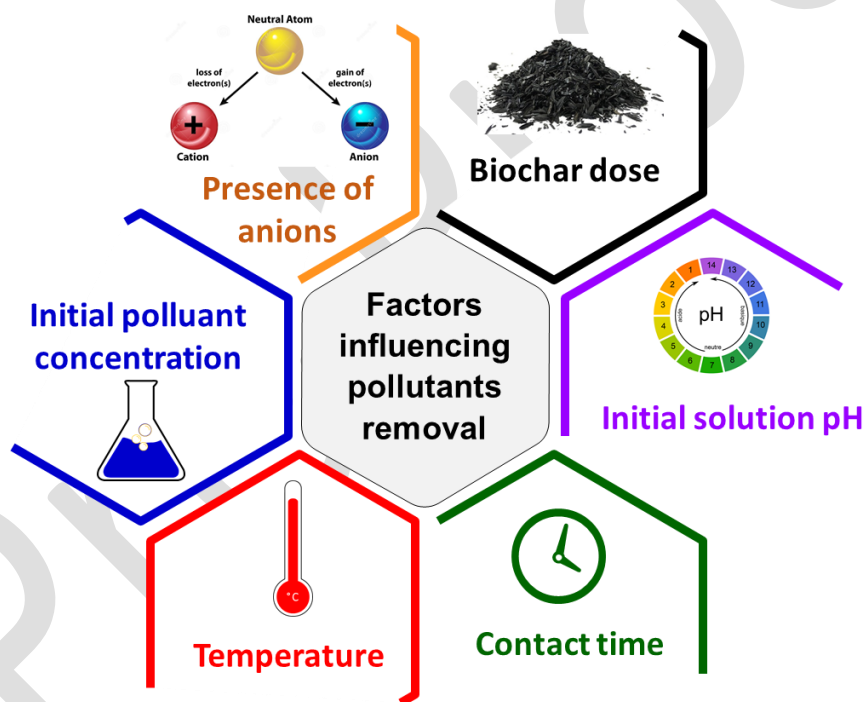
412 Other potential risks of biochar are due to adsorbed pollutants on the biochar surface, the
413 presence of residual chemicals in biochar originating from the plant residues persisting
414 the pyrolysis process, and finally the leaching out of various components from the
415 biodegradation under natural conditions of aged biochar [119].

416 The voluntary biochar quality standards that apply in Europe with the European Biochar
417 Certificate (EBC) [120], in the UK with the biochar quality mandate (BQM) and in the USA
418 with the International Biochar Initiative-Biochar Standard (IBI-BS) propose limits for
419 certain harmful components in biochar such as; PAH, benzo (a) pyrene, polychlorinated
420 biphenyls (PCBs), polychlorinated dibenzodioxins (PCDDs), polychlorinated
421 dibenzofurans and heavy metals [120][121]. However, these standards are safeguarding
422 biochar production rather than final applications, therefore prior to applying novel
423 adsorbents with potential ecotoxic effects the national safety regulations for air, soil and
424 water need to be secured at all times.

425

426 **4. Factors influencing pollutants removal**

427 The elimination of pollutants and the adsorption capacity of biochar are greatly affected
428 by its physicochemical properties as well as of the target pollutants nature, and the
429 operating conditions of the treatment, as reported in Tables 1 and 2 [122]. Several works
430 report the effect of different parameters and their interaction on the removal efficiency of
431 pollutants with the help of multivariate optimization approach [123][124]. Figure 3 shows
432 the factors influencing the removal of organic pollutants by biochar. In general, biochar
433 concentration and initial pH of the solution are the most discussed.



434
435 **Figure 3:** The main influencing parameters in organic pollutants removal by biochar.
436

437 **4.1. Effect of biochar dose**

438 The impact of biochar dose on pollutant removal efficiency is reported in detail in most of
439 the adsorption studies, because of the high correlation observed between adsorbent
440 dosage and adsorption capacity. However there is an optimum value of biochar dose,
441 beyond this threshold there is no enhancement in the pollutant elimination anymore [42].
442 This tendency is explained by the optimum use of the active adsorption sites for pollutant
443 adsorption [125]. Beyond the optimum point, the decrease in the adsorption capacity may
444 be due to the inadequate availability of pollutant molecules for spare active sites [126]. In
445 another study the increased biochar quantity results to a faster achievement of the
446 reaction equilibrium, indicating the increased availability of vacant reactive sites on the
447 adsorbent surface, which leads to a high adsorption rate at the beginning of the process
448 [127]. However the increase in biochar dosage decreases the adsorption capacity
449 exponentially but moderately at lower dosages and slightly at higher dosages [128].

450

451 **4.2. Effect of initial solution pH**

452 The pH of pollutant solution is a factor which influences the removal efficiency because of
453 the predominant role on the charge characteristics through the protonation and
454 deprotonation of oxygen-containing groups on the biochar or biochar composite surface
455 [129]. The pH value also influences the degree of ionization of the adsorbate [130]. Wang
456 et al reported that anion adsorption is favored at pH less than the point of zero charge
457 (PZC) because the adsorbent surface is positively charged. However, when the surface
458 is negatively charged at pH values above the PZC the cation adsorption is favored [131].

459 In the work of Chaukura et al, a maximum adsorption of methyl orange was recorded at
460 pH value lower than the PZC of biochar, this was explained by possible electrostatic
461 attraction of the dye molecules to biochar surface since the dye molecules existed as
462 anions at the reported conditions [132]. Generally, the organic dyes adsorption capacity
463 by biochar or nano-metal biochar composites decrease with increasing solution pH values
464 [133].

465 **4.3. Effect of pollutant concentration**

466 The initial concentration of the adsorbate plays a crucial role in the efficiency of the
467 adsorption process. It is reported that the adsorption capacity decreases with the increase
468 in the initial concentration of pollutants [134]. This is attributed to the occupation of active
469 sites on the adsorbent material surface by the targeted pollutants [127]. Some works
470 reported a proportional relationship between pollutant initial concentration and adsorption
471 capacity of biochar; however, the removal yield of pollutant decreases [135][136]. An
472 explanation of this can be that at higher concentration, the mass transfer driving force
473 increased [85], which enhanced the diffusion rate and the probability that molecules
474 reached the material surface increases [137]. We would like to comment that if the
475 diffusion rate is enhanced, one may observe positive correlation between concentration
476 and rate of adsorption, instead of adsorption capacity [135][136], as the latter should be
477 dependent of the total available sorption site amount on biochar.

478 Sayin et al. reported a decrease of adsorption efficiency with increasing the ciprofloxacin
479 initial concentration from 50 to 150 mg/L, and this was explained by the gradual saturation
480 of specific active site for antibiotic molecules adsorption [138]. Nnadozie and P.A. Ajibade

481 studied the adsorption of Indigo Carmine (IC) dye using *C. odorata* biochar, the result
482 showed a decrease in the removal efficiency with increasing dye concentration from 10 to
483 100 mg/L with the same biochar dose [139].

484 **4.4. Effect of anions presence**

485 The pollutant molecules may compete with various coexisting anions such as NO_3^- , Cl^- ,
486 SO_4^{2-} and PO_4^{3-} during adsorption in aqueous environment. Wang et al reported a
487 decrease in the removal efficiency of p-arsanilic acid in the presence of PO_4^{3-} because of
488 the stronger competitiveness for the adsorptive sites on the surface of biochar [140]. The
489 increase in NaCl content decrease the adsorption capacity of biochar [54], which was
490 explained by the reduction of repulsion force between adsorbent particles and hence the
491 increase of aggregation of nanomaterials [141]. However, beyond a certain dose of NaCl
492 increase, the adsorption capacity increases, which was attributed to the increase of ionic
493 strength which improved the activity coefficient of hydrophobic organic compounds,
494 resulting in a decrease in solubility (i.e. salting-out effect), thus was conducive to pollutant
495 adsorption [142]. It can also be explained by surface charge neutralization of the
496 carbonaceous adsorbents by the double layer compression and the reduced solubility of
497 the micropollutants in the presence of high Na^+ concentration [82].

498 **4.5. Effect of contact time**

499 The effect of contact time needs to be considered in the evaluation of the biochar
500 adsorption system. Published research reports a fast increase in the adsorption capacity
501 at the beginning of the treatment and a gradual slow-down of the adsorption capacity until

502 adsorption equilibrium is reached, when the sorption sites were fully occupied [135][143].
503 This can be explained by the gradual adsorption saturation of active sites on biochar and
504 the gradual decrease in the differential concentration between solution bulk phase and
505 the surface of the adsorbent [144]. Similar results were observed by Velusamy et al. [145]
506 and Li et al., in the removal of ciprofloxacin [146]. Sayin et al., in their work on the removal
507 of ciprofloxacin by H₃PO₄ modified biochar, reported the decrease of the adsorption rate
508 of antibiotic molecules with increasing time of treatment and that until the equilibrium point
509 of time [138]. Nguyen et al. in their study tested diverse Metal salt-modified biochars
510 derived from different agro-waste for the removal of Congo red dye. The results revealed
511 the different equilibrium times needed for the different biochars applied at the same initial
512 concentration of the dye [13].

513 **4.6. Effect of temperature**

514 The adsorption temperature can also affect the pollutants removal capacity by biochar
515 and its composites. However, the majority of water treatment experiments are conducted
516 at ambient temperature (25 °C) to simulate the temperature predominant in the
517 environments [147]. It is reported that the adsorption increases with increasing
518 temperature in the range of 15-35°C [71], which reflects an endothermic process [148].
519 Similar results on the endothermicity of : i) p-nitrophenol adsorption by pine sawdust
520 biochar was reported in the work of Liu et al [149] and ii) diclofenac adsorption by pine
521 wood biochar [150]. The increase in temperature increased the probability of pollutant
522 molecules contacting the active sites [148]. However, the increase of temperature in the
523 same range can reduce the adsorption capacity in an exothermic process [136][145]. On

524 the other hand there is a proportional relationship between temperature and the molecular
525 movement acceleration, which promotes adsorbent-ion interaction and reduction of the
526 Gibbs free energy [151][152]. The increase of temperature can enhance the formation of
527 aromatic carbon present on the surface of biochar resulting to improved surface
528 characteristics for adsorbing an extensive range of pollutants [153].

529 **4.7. Effect of chemical impregnation ratio on the removal of pollutants**

530 The ratio of the non-processed to magnetic material was studied in several works to
531 evaluate its effect on pollutant removal efficiency. It is found that the increase of this ratio
532 increases the adsorption capacity of magnetic biochar until an optimum value but further
533 increase leads to a decrease of the adsorption capacity [154]. However, Son et al report
534 that copper removal capacities decrease with decreasing biochar/Iron ratio and Fe
535 recovery efficiency, explained by the plugging of biochar's surface pores with iron oxide
536 particles [155]. In addition, Yang et al. found that the increase in FeCl_3 /sawdust
537 impregnation mass ratio increases the removal efficiency of mercury which was attributed
538 to oxygen-rich functional groups formation at biochar surface and especially C=O group.
539 However, an excess of FeCl_3 can lead to; i) the aggregation of Fe_3O_4 particles on the
540 magnetic biochar surface, and/or ii) the variation of textural properties and therefore a
541 decrease in mercury removal yield [156].

542 **5. Post-processing modification of biochar: Activation and functionalization**

543
544 The thermal decomposition of biomass in the absence of oxygen, or at very limited oxygen
545 environment, produces biochars that still contain various refractory oxides, depending on

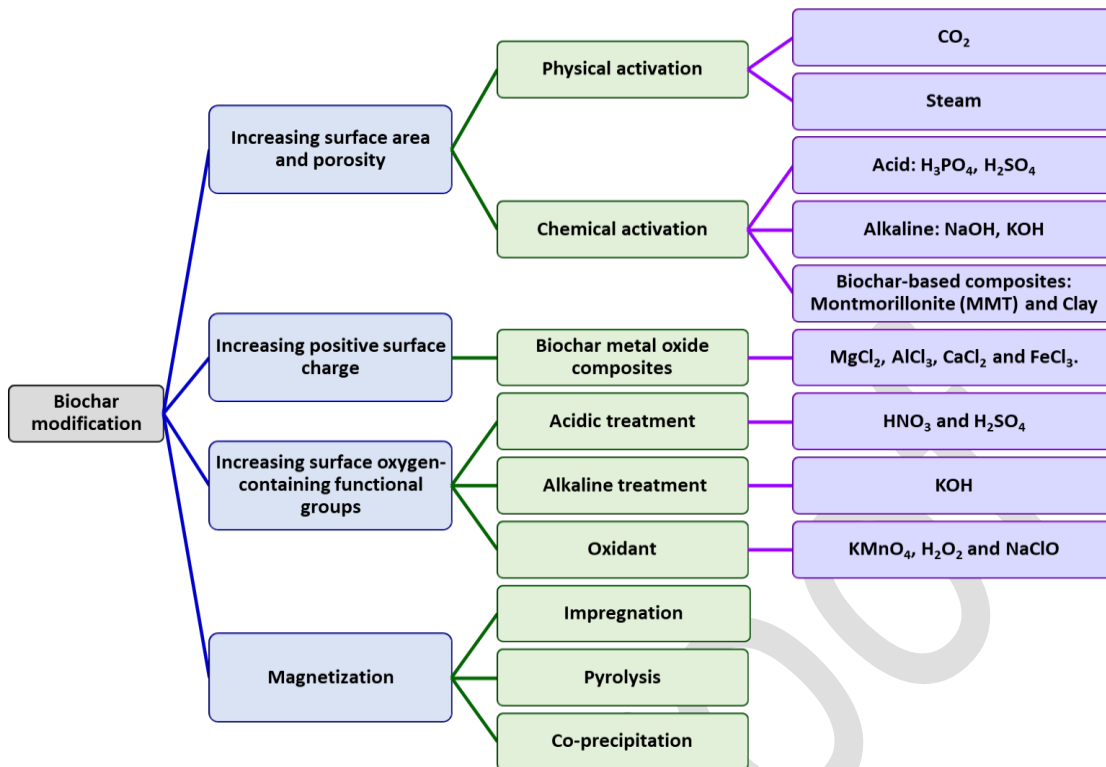
546 the biomass feedstock, such as Fe_2O_3 , SiO_2 , KCl , Al_2O_3 , CaSO_4 , CaCO_3 [157].
547 Furthermore, the surface of most pristine biochars are often negatively charged in
548 association with its abundant oxygen-containing function groups, thus exhibiting specific
549 sorption to cations (e.g., heavy metals ions) [158]. However, sorption toward anionic
550 species (i.e., oxyanion, anionic dyes and organics) is limited [159]. This limits the
551 applications of biochar which drives researchers to introduce new and additional metal
552 oxides with different methods to modify biochar for targeted applications [160].

553 In addition, biochar prepared by conventional pyrolysis of biomass may have poor
554 physicochemical properties such as surface oxygenated groups, surface area, pore
555 volume, and pore width. These properties fluctuate considerably and depend on feedstock
556 types and production conditions [161]. Nevertheless, the available functional groups
557 (carboxyl ($-\text{COOH}$), hydroxyl ($-\text{OH}$), and carbonyl ($\text{C}=\text{O}$)), are quite important in water
558 treatment [162]. The hydrophilic (polarity index) or hydrophobic property (aromaticity) of
559 biochar highly depends upon the type and nature of existing functional groups on the
560 surface. Different techniques available have been reported to boost the abundance of this
561 last, such as steam activation, impregnation method, chemical and heat treatments [163].

562 Biochar can also act as an excellent photocatalyst when combined with other catalysts,
563 because of the resulting favorable physicochemical properties such as; high surface area
564 with high active site, enhanced charge separation, higher availability of functional groups,
565 high porous volume, better catalyzing ability, stability and recoverability [164]. However,
566 the synthesis of photocatalyst-based biochar must be optimized [165]. As reported by Yu
567 et al., the addition of an appropriate amount of ZnO into biochar enhanced both the
568 adsorption capacity and the photocatalytic ability of the nanocomposites [46]. Similar

569 results were reported in the application of Mn-loaded and Fe-loaded biochar for the
570 atrazine elimination in aqueous solution with heterogeneous catalytic ozonation [166].
571 Ahmaruzzaman reported a different synthesis technique of biochar supported
572 photocatalyst like Sol-gel method, Ultrasound assisted synthesis, Thermal
573 polycondensation technique, Solvothermal process, Hydrothermal process [164].

574 As seen in the Figure 4, the different post-modification methods of biochar are classified
575 into four main categories; 1) modifications to increase the surface area and porosity; 2)
576 modifications to render the biochar surface positively charged; 3) Increasing surface
577 oxygen-containing functional groups and 4) magnetization of biochar in order to
578 facilitate/enhance the biochar particles recovery. It may be that one treatment can
579 enhance two or more properties at the same time, for example the case of H₂SO₄
580 treatment which enhances the specific surface area and increases the oxygen-containing
581 functional groups. There are different classifications for these modifications reported in
582 literature [167][18] such as the classification according to physicochemical characteristics
583 of biochar targeted by the modification [161], or according to the nature of process
584 (chemical, physical or composite) [168].



585

586

Figure 4: Typical engineered biochar modifications and its classification.

587

588

589

590

591

592

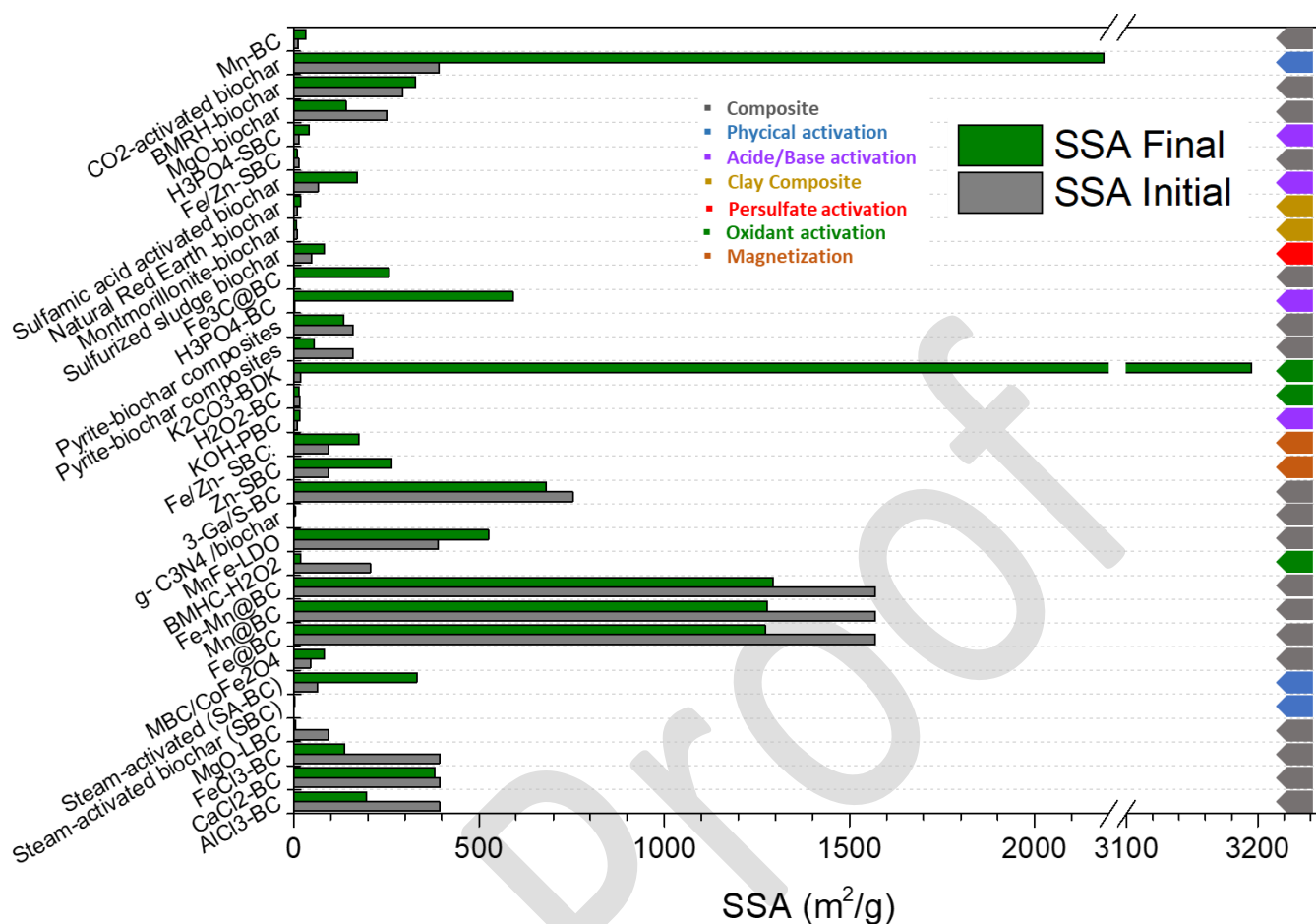
593

594

595

596

Figure 5 shows the effect of different modification treatments on the biochars' specific surface area (SSA) as reported in literature. We observe that: i) the result for a treatment technique varies from one biochar to another (case of Mn-BC modification and H₃PO₄ treatment for example); ii) some treatments lead to a decrease in SSA (case of FeCl₃-BC and AlCl₃-BC); iii) some techniques presented a considerable increase in the SSA such as CO₂ activation and K₂CO₃ treatment. The Increase of biochar SSA resulting from different posttreatment techniques does not always mean the improvement of its performance towards the removal of organic pollutants.



597

598

599

600

601

Figure 5: The evolution of specific surface area (SSA) of biochar according to different modification techniques in some reported works ([13], [169], [170], [171], [172], [173], [77], [174], [175],[76],[75],[90],[90],[56],[86],[69],[176],[177],[39],[178], [179],[180], [52], [64]).

602

603

604

605

606

607

Moreover, as reported in detail by Barquilha and Braga, organic and inorganic pollutants adsorption on biochars can involve different mechanisms, including physical and chemical interactions. The interaction between biochars and adsorbate species is not simple and may involve different adsorption mechanisms, such as van der Waals forces, electrostatic interactions, surface complexation, ion-exchange, hydrophobic interactions, π -interactions, co-precipitation, partition, and pore-filling [181]. Other studies report on the

608 mechanisms of dye adsorption by sewage sludge-biochar [182] and adsorption
609 mechanisms of modified biochar on typical emerging contaminants [167].

610

611 **5.1. Acid-base activation/decoration**

612

613 Generally, biochar modification by acidic treatment occurs in two main ways: activation
614 and decoration. Activation is to develop porous structure and increase specific surface
615 area by using chemical activating agents with highly etching ability. Whereas, decoration
616 emphasizes on enhancing surface activity, by using zero-valent iron nanoparticles [183],
617 Fe_3O_4 and FeOOH as additives [184]. Another work reported the enhancement of sorbent
618 hydrophobicity by decoration with different acid and fatty acids such as; pure lauric acid,
619 acetic anhydride, phosphoric acid and citric acid [185][186][187].

620 Gurav et al., reported the application of pinewood biochar decorated with coconut oil-
621 derived fatty acids for adsorptive removal of crude petroleum oil from water. Fatty acids
622 composition attached to the resulted biochar (mg/g of biochar) was reported as: lauric acid
623 (9.024), myristic acid (5.065), palmitic acid (2.769), capric acid (1.639), oleic acid (1.362),
624 stearic acid (1.114), and linoleic acid (0.130). Decorated biochar presented a higher
625 hydrophobicity and a good reusability with stable adsorption efficiency at 51.40% after fifth
626 adsorption-desorption cycles [188]. The sulfamic acid modified biochar reported in the
627 work of Liu et al., presented a specific surface area with 2.6 times larger than that of the
628 original biochar introducing more functional groups on the biochar. Furthermore, the
629 resulted biochar shows an improved performance for tetracycline adsorption [39].

630 Many studies have proved that biochar treated with a strong oxidizing agent (e.g.,
631 $\text{HNO}_3/\text{H}_2\text{SO}_4$, HNO_3 , HF/HNO_3 , KMnO_4 , H_2O_2 and NaClO) enhance its sorption capacity,

632 creates charged and hydrophilic surface functional groups, and increases their colloidal
633 stability and mobility [189]. The activation of biochar in one step and two steps by KOH
634 and KMnO_4 as a green activator was found to give a large pore volume, pore channel and
635 proportion of aromatized structure, it revealed to have a high adsorption capacity for
636 methylene blue removal [190]. The oxidation of corncob biochar by of $\text{HNO}_3\text{-H}_2\text{SO}_4$
637 mixture was found to boost the adsorption capacity of biochar, decrease hydrophobicity
638 and increase the amounts of oxygen-containing groups [191]. The treatment of sludge
639 biochar modified by $\text{Fe/Zn} + \text{H}_3\text{PO}_4$ presented an adsorption capacity for ciprofloxacin
640 (CIP), norfloxacin (NOR) and ofloxacin (OFL) from water up to 20 times of those of sludge
641 biochar only or H_3PO_4 modified biochar [178].

642 Some works reported the NaOH activation of biochar or biomass before pyrolysis in order
643 to well-developed mesoporous structure [192], enhance the higher specific surface area,
644 total pore volume, aromaticity [193], and graphitized orderly carbon layer in biochar [135].
645 The KOH treatment was also reported to increase the surface area and pore volume [194].
646 Apparently, biochar modification with a strong inorganic acid is one of a simple and
647 effective processes for biochar activation. However, the scaling-up into an industrial scale
648 will produce a large amount of acidic or basic wastewater, with negative impact to the
649 aquatic environment.

650 **5.2. Persulfate activation**

651
652 Persulfate (PS) activated biochar was reported in many studies in the last years
653 [173][195], due to the increased pollutant removal efficiency from water by combining the
654 advantage of PS radicals effect and the high specific surface area of biochar [196][197].

655 It is noticed that, compared with the traditional hydroxyl radical-based AOP, Sulfate
656 radicals-AOP has a higher redox potential (2.5–3.1 V ($\text{SO}_4^{\cdot-}$) vs. 2.7 V ($\cdot\text{OH}$)), but longer
657 half-life time (30–40 μs ($\text{SO}_4^{\cdot-}$) vs. $<1 \mu\text{s}$ ($\cdot\text{OH}$)) and wide pH adaptability [198]. Fan et al.
658 reported the slight adsorption of bisphenol A (8.1%) by sludge-derived biochar (SBC)
659 alone and limited direct oxidation (2.4%) by sole peroxymonosulfate (PMS), nevertheless,
660 the removal efficiency of bisphenol A was boosted to 94.5% within 60 min in the presence
661 of both SBC and PMS. that the explanation is that PMS is bound to SBC and forming a
662 surface reactive complex (SBC-PMS*), which would abstract the electrons from the
663 adsorbed pollutant through the conductive carbon tunnel [199].

664 Furthermore, different biochar modification options can be combined to promote the
665 elimination of aqueous pollutants, such as magnetization and peroxymonosulfate (PMS)
666 activation, reported by You et al. [172].

667

668 **5.3. Physical activation**

669

670 Physical activation of biochar is the partial oxidation of the material to increase its porosity,
671 under low to medium heat treatment ($<250^\circ\text{C}$) under air conditions or high temperature
672 ($>750^\circ\text{C}$) treatment with CO_2 , steam, blends thereof. At high temperatures H_2O and CO_2
673 become reactive and therefore allow for chemical reactions with the biochar matrix [200].
674 Jellali et al. reported the increase of the surface area and total pore volume after CO_2
675 activation by about 5.9 and 1.5 times, respectively [122]. Meanwhile the activation process
676 with air at a low temperature ($\approx 275^\circ\text{C}$) for 4 h significantly enhanced the structure and
677 texture of the biochar generated from different sewage sludge types [201]. Sewu et al.
678 reported that the steam activation of biochar enhances the porosity and increases the

679 specific surface area by 5 times and the adsorption capacity of crystal violet by 4.1 time
680 [171]. Similar results were reported by Wang et al. for the synergistic removal of Cu^{2+} and
681 tetracycline (TC) with steam-activated bamboo-derived biochar [170]. Ibrahim et al
682 reported that steam activation of carbonized Oil Palm Mesocarp Fiber presents a high
683 removal of the chemical oxygen demand and suspended solids from 395 mg/L and 117
684 mg/L to 122 mg/L and 7 mg/L, respectively in a treated wastewater after 6 consecutive
685 treatment cycles [202]. Some works reported that alkali and steam treatments can be used
686 to increase porosity and clean blocked pores [203][204].

687

688 **5.4. Biochar-based composites**

689

690 It is reported that producing biochar-based composites allows to combine the advantages
691 of biochar with nano-materials, where the resulting composites usually exhibit great
692 improvement in functional groups, pore properties, surface active sites, adjusted net
693 surface charges, catalytic degradation ability and easy for recovery [204][180]. These
694 composites can be classified into three categories based on their synthesis process
695 towards biochar-based nano-materials; i) nano-metal oxide/hydroxide-biochar
696 composites, ii) magnetic biochar composites [159], and iii) clay mineral based-biochar
697 [205].

698

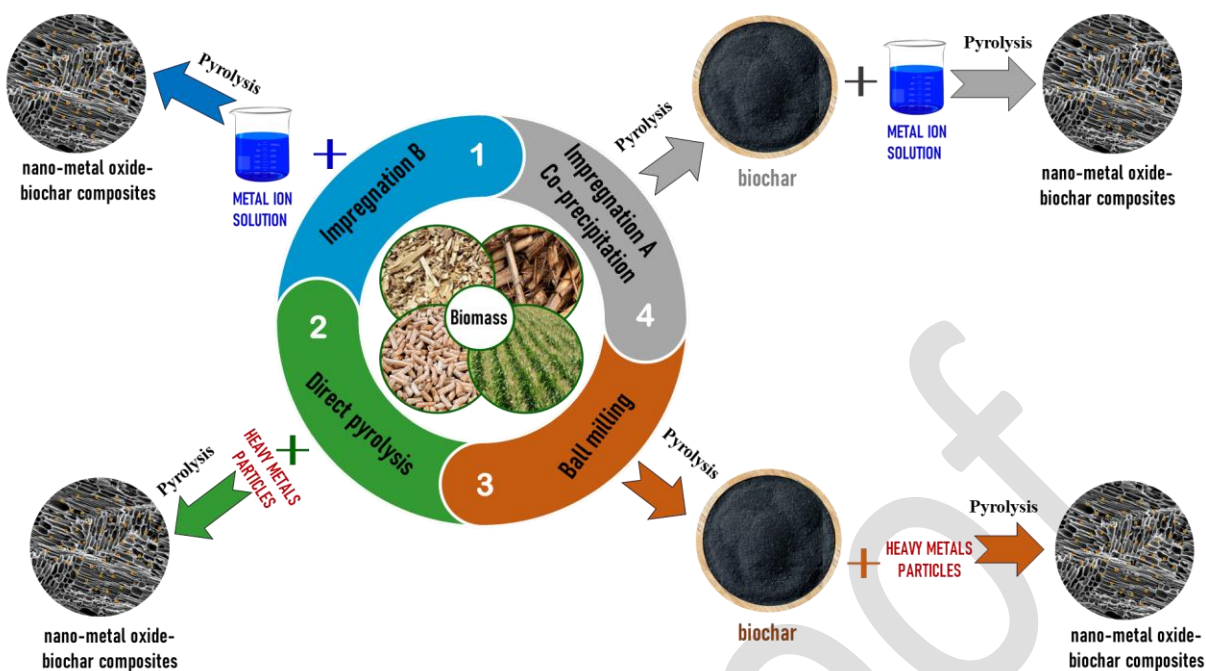
699 **5.4.1. Nano-metal oxide/hydroxide-biochar composites**

700

701 Several chemical additives have been used in the synthesis of these composites, like
702 H_3PO_4 , NaCl, K_2CO_3 , MgCl_2 , ZnCl_2 , KOH, CaCl_2 and FeCl_3 , which may be added before

703 or after biomass carbonization [161], in powder forms or dissolved, as shown in figure 5.
704 Table 6 summarizes some works reported on nano-metal oxide- biochar composite
705 synthesized to treat organic pollutants, where it can be seen that there are different
706 preparation methods for these composites under diverse operating conditions. So, for
707 example we find co-precipitation, pyrolysis, impregnation, sol-gel method and chemical
708 reduction. Using a different classification method, in their review Zhao et al classified the
709 nano-metal oxide-biochar composites preparation into four methods as presented in the
710 figure 6; i) Impregnation which is characterized by its simplicity and a large capacity of
711 obtained composites, ii) Chemical coprecipitation characterized by low cost, high purity,
712 homogeneous nanoparticles, both these methods have the disadvantage of causing
713 chemical pollution, iii) direct pyrolysis characterized by the easy preparation and the prior
714 biomass enriched with target heavy metals but it is difficult to control the nano-metal
715 oxides/biochar ratio in the composites, iv) Ball milling with various advantages like Low
716 cost, easy to operate, no chemical pollution, effective reduction of particle size of metal
717 oxides. In the downside, during the ball milling preparation particles are easily dispersed
718 in water and move to surface runoff, pollutants can migrate out of the contaminated site,
719 posing potential risks to groundwater [133].

720



721
722
723 **Figure 6:** Different pathways for Nano-metal oxide/hydroxide-biochar composites
724 synthesis.

725
726 Special attention is given to the ball milling technique, during which samples including
727 biochars are crushed to nanometer size in the presence of metal oxide particles [206].
728 Ball milling has the capacity to increase the SSA, probably by revealing pores [207], and
729 to increase the oxygen-containing functional groups (e.g., carboxyl, lactone, and hydroxyl)
730 [208]. Zheng et al. developed a new ball-milling process to synthesize MgO/biochar
731 nanocomposites with a dual- functional adsorbent to remove both cationic and anionic
732 pollutants. The developed materials enhanced the adsorption of methylene blue (MB) for
733 about 8.4 times, likely due to increased surface area and pore volume [179].

734
735 **Table 6:** Reported work on Nano-metal oxide-biochar composites synthesis for organic
736 pollutants removal.

Biochar	Synthesis method	Reagent	Operating Conditions	Reference
MnOx-coated rice straw biochar	Co-precipitation	KMnO ₄	The mixed solution was vibrating continuously at 30 °C for 8 h and then oven-dried at 80 °C for 24 h after washing.	[129]
Fe ₂ O ₃ – Paper and pulp sludge biochar	One-step pyrolysis	FeCl ₃	Pyrolysis of FeCl ₃ -impregnated Paper and pulp sludge (1:3, m/v) at 750 C for 2 h in a one-step pyrolysis method.	[132]
Mg-biochar, Al-biochar, Fe-biochar and Ca-biochar	Pyrolysis (impregnation)	MgCl ₂ .6H ₂ O, AlCl ₃ .6H ₂ O, CaCl ₂ .2H ₂ O and FeCl ₃ .6H ₂ O	A dry mixture of biomass and MgCl ₂ (or AlCl ₃ , CaCl ₂ , FeCl ₃) was heated at 10 C/min up to 600 C under N ₂ flow for 1 h.	[147]
Nano-MgO modified fallen leaf biochar	Sol-gel method	MgCl ₂ .6H ₂ O	MgCl ₂ .6H ₂ O mixed with biochar suspension, stirred at 25 °C for 6 h and then centrifuged and dried at 80°C	[169]
AlCl ₃ - agro-waste biochar, FeCl ₃ - agro-waste biochar,	Pre-pyrolysis treatment	AlCl ₃ .6H ₂ O, FeCl ₃ .6H ₂ O, and CaCl ₂	Biochar added to salt solution, stirred (ambient Temperature for 24h),	[13]

CaCl ₂ - agro-waste biochar	followed by pyrolysis		filtered, dried at 80°C and the pyrolyzed at 500 °C.	
Nano-zerovalent manganese/biochar composite (nZVMn/PBC)	Chemical reduction method	MnCl ₂ , NaBH ₄	MnCl ₂ was dissolved in water and ethanol mixture, biochar was added simultaneously, NaBH ₄ was added drip by drop to the mixture, and then sonicated, followed by water remove and drying.	[68]

737

738 Finally Sewu and his co-workers reported that using non-magnetic goethite mineral (α -
739 FeOOH) in co-pyrolysis with firwood biomass to produce biochar proved as a green
740 process when compared to the ubiquitous and conventionally used FeCl₃, which has a
741 negative impact due to toxicity [209].

742

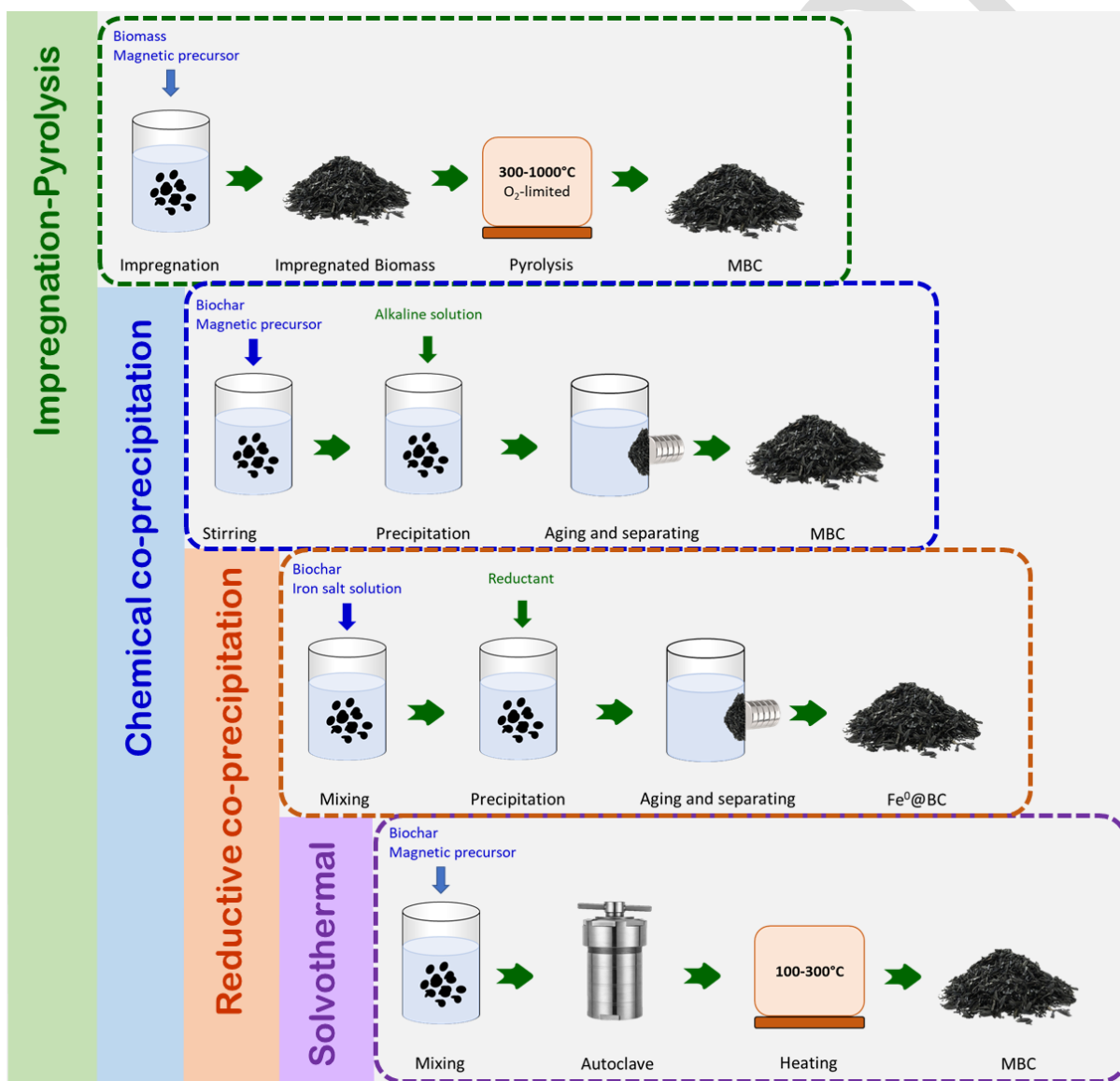
743 **5.4.2. Magnetic biochar composites**

744

745 Significant research efforts have been carried out to improve the adsorption capacity of
746 biochar. However, due to the small particle sizes and lower density, the separation and
747 reuse of biochar after water pollutants elimination remain one of the main problems to be
748 resolved [210]. Magnetic biochar has been successfully produced by various methods as
749 reported in literature [211], presented in figure 7, showing the impregnation-pyrolysis,
750 chemical co-precipitation, solvothermal and reductive co-precipitation methods. It is
751 shown that these biochar composites provide effective absorptivity, ready separation by

752 using external magnets and easy recycling [212]. Nevertheless, the traditional loading-
753 process of magnetic medium increases the cost of the sorbent [213]. Thines et al reported
754 three main common techniques employed to produce magnetic material such as pyrolysis,
755 co-precipitation and calcination method [214]. An additional common production method
756 was reported in literature such as, conventional heating in an electrical furnace [215],
757 microwave heating in a modified furnace [216][154].

758



759

760 **Figure 7:** Schematic diagram of common Magnetic biochar preparation methods.

761
762 The co-precipitation method was found to be the simplest due to its easy step of mixing
763 and heating. This process focuses on the molar ratio of transition metal's ion being used
764 during the mixing for improving the characteristics of the magnetic biochar produced, in
765 terms of magnetism and porosity [214]. Co-precipitation methods result to coating the
766 surface of biochar with different iron oxides such as, Fe_3O_4 , $\alpha\text{-Fe}_2\text{O}_3$, and CoFe_2O_4
767 particles, which give magnetic proprieties for active sites of iron oxide for pollutant
768 elimination [212][217][218].

769 It has been reported that additives with a high decomposition capacity (e.g., AlCl_3 , FeCl_2
770 and MgCl_2) exhibits catalytic activity, higher sorption capability, increasing porosity and
771 creating positively charged adsorption sites [161][219][220]. Table 7 summarizes some
772 results on the preparation of magnetic biochars following different synthesis pathways,
773 different metal reagents and different operating conditions.

774
775 **Table 7:** Literature on magnetic biochar composites synthesis for organic pollutants
776 removal.

Magnetic biochar	Synthesis method	Reagent	Operating Condition	reference
Magnetic activated sawdust hydrochar	Slow thermal pyrolysis	$\text{Fe}(\text{NO}_3)_3$	Pyrolysis under N_2 flow for 1h at 700°C with with a heating rate 3 K min^{-1} .	[221]

Cottonwood biochar/ γ - Fe_2O_3	Thermal pyrolysis	Ferric chloride hexahydrate, $\text{FeCl}_3 \cdot 6\text{H}_2\text{O}$	Biomass were immersed into FeCl_3 solution for 2 h and dried at 80 °C for 2 h followed by pyrolyzing the biomass mixture in a furnace at 600 °C with the flow of N_2 for 1 h.	[222]
Fe_3O_4 -loaded hydrochar magnetic biochar	Thermal pyrolysis	$\text{FeCl}_3 \cdot 6\text{H}_2\text{O}$ and ZnCl_2	Pyrolysed under N_2 flow of 1 L/min for 30 min at a temperature range of 500°C to 800°C	[223]
Humic acid coated magnetic biochar	Thermal pyrolysis	$\text{FeCl}_3 \cdot 6\text{H}_2\text{O}$ and humic acid	Pyrolysis with a heating rate of 20 °C min^{-1} at 500 °C for 6 h. humic acid and magnetic biochar obtained was stirred at 25 °C with 170 r min^{-1} for 24 h and kept quiescent for 48 h.	[224]
Magnetic greigite/biochar composites	Co-precipitation /solvothermal method	$\text{FeSO}_4 \cdot 7\text{H}_2\text{O}$	Suspension was heated at 180 C for 12 h.	[225]

CuFe ₂ O ₄ -loaded magnetic biochar	Co-precipitation process	CuCl ₂ and FeCl ₃	Process were carried out at pH10 and the suspension were heated to 98–100 °C for 2 h. Molar ratio of 1:2 of Cu ²⁺ : Fe ³⁺ .	[226]
Fe and Mn ions onto pinewood biochar	Co-precipitation process	MnCl ₂ ·4H ₂ O and FeCl ₃ ·6H ₂ O	Under N ₂ flow, reaction of suspension for 4 h at 80 °C. Then resulting biochar dried at 80 °C for 12 hours.	[227]
Ca-Mg/biochar	Co-precipitation process	MgCl ₂ and CaCl ₂	Corncob was suspended in MgCl ₂ (ratio of 1:3) and CaCl ₂ (ratio of 1:3) and were further heated under N ₂ flow.	[228]
Magnetic modified sugarcane bagasse (MSCB)	Co-precipitation process	FeCl ₃ and FeSO ₄	Mixture dissolved in an ammonia solution and proceed with ultrasound irradiation at 60°C. Molar ratio of Fe ³⁺ : Fe ²⁺ is 1:2	[229]
Fe ₃ O ₄ -loaded bentonite magnetic biochar	Calcination process	FeCl ₃ ·6H ₂ O	Calcined at 190°C for 8 h.	[230]
Fe ₃ O ₄ -loaded microalgae magnetic biochar	Calcination process	FeSO ₄ ·6H ₂ O	Calcined at different temperatures for 6 h.	[231]

778 **5.4.3. Clay mineral modification**

779
780 Clay-biochar composite is the result of pre-mixing the raw biomass before pyrolysis or the
781 post mixing of produced biochar with clay minerals [232]. The synthesis methods,
782 characteristics of clay minerals-biochar and the surface interactions with contaminants
783 during treatment has been reviewed by Arif et al [205]. This composite is characterized by
784 high porosity and a great compatibility with water pollutants [233]. Premarathna, et al.
785 reported the synthesis of a novel clay-biochar composite from montmorillonite (MMT) and
786 red earth (RE) clay materials with municipal solid waste (MSW) biochar in pyrolysis. The
787 obtained composites exhibit a high adsorption capacity towards removing tetracycline
788 antibiotic in aqueous media [234]. Similar results were reported by Borthakur et al. for
789 tetracycline removal from wastewater [177]. It is noticed that the surface properties of the
790 biochar samples are considerably affected by the incorporation of different clay material.
791 Zhao and Zhou revealed that clay-mineral modification enhanced the micro-pore area of
792 biochar by more than 200% while only a slight growth in the mesopore area was observed
793 [235]. It is also reported that organo-mineral layer of clay increases the biochar stability
794 and its ability to resist the process of decomposition when biochar is applied to soil [236].
795 From a mechanistic point of view, interactions of BC-clay/mineral composites with
796 inorganic and organic contaminants can be established according to different
797 mechanisms including ion exchange, physical adsorption, precipitation, complexation,
798 electrostatic interaction, H-bonding, partitioning, electron-donor-acceptor (EDA)
799 interaction, hydrophobic interaction and pore-filling [237].

800 **6. Biochar applications for organic pollutants removal from water**

801 **6.1. Adsorption**

802
803 There is a high research interest in the adsorption as a technique for mineral and/or
804 organic contaminated water treatment, reflected by the high number of publications in the
805 area [238][239][240]. Lu et al. reported the simultaneous elimination of metal ions and
806 organic compounds from aqueous solutions by rice bran, bamboo and their derived
807 biochars. These biochars presented a high sorption capacity for acenaphthene removal
808 compared to the original biomass whereas the coexisting Cu^{2+} and Cr^{+6} both inhibited the
809 sorption of acenaphthene by the biochar [136]. Similar results were reported by Cheng et
810 al. for the adsorption of methyl orange in the presence of Cr^{6+} from dye wastewater [71].
811 The simultaneous removal of toxic $\text{Pb}(\text{II})$ ions, poly(acrylic acid) and Triton X-100 from
812 their mixed solution was achieved by using engineered acid activated biochars obtained
813 from horsetail herb precursor [241]. Shin et al. investigated the competitive adsorption of
814 three pharmaceuticals; naproxen (NPX), diclofenac (DCF), and ibuprofen (IBU) from lake
815 water and wastewater effluent. The results revealed that the competitive adsorption of
816 NPX, DCF, and IBU for the NaOH-activated SCW biochar was more spontaneously endo-
817 thermic than that for the pristine SCW biochar [193].

818

819 **6.2. Filtration**

820
821 The filtration technique was also studied and tested for the removal of different pollutants
822 from wastewater. Wang et al., reported the removal of microplastic spheres by different
823 biochar filters in a column system. In their study, biochar was packed in a 7 cm height bed

824 between two sand layers of 3 cm height each. The results show that the biochar filters
825 provide significant capacity for the removal and immobilization of 10 μm diameter
826 microplastic spheres (more than 95% removal efficiency) which is much higher than that
827 of similar grain-sized sand filter studied [242]. Biochar can also be used for the pathogens
828 removal (such as *Escherichia coli* and *Enterococc*) of as a common sand filter [243].
829 Kaetzi et al, studied the elimination of organic pollutant from raw sewage by using
830 Miscanthus-biochar based filter media. Some works reported that the filtration removal is
831 more dominant than adsorption where the result showed $74 \pm 18\%$ of chemical oxygen
832 demand (COD) removal by biochar filters when only $61 \pm 12\%$ of COD reduction was
833 recorded for sand filters [244]. Reddy et al., have used a filtration column with an inner
834 diameter of 7 cm and a length of 61 cm for the elimination of different contaminants from
835 urban storm water runoff. The results proved that biochar-filter reduced the total
836 suspended solids (TSS), nitrate, phosphate and polycyclic aromatic hydrocarbons (PAHs)
837 by an average of 86%, 86%, 47% and 68%, respectively [245].

838

839 **6.3. Coupled Adsorption and advanced oxidation processes (AOPs)**

840

841 Recently, the application of biochar (BC)-based composite materials in catalytic oxidation
842 treatment has been proposed for organic contaminants elimination and degradation
843 [245][246]. The introduction of these composites in the AOPs is due to the dual benefits
844 of adsorption and catalytic degradation [247]. Huang et al. revealed that morphological
845 and chemical features of biochar played an important role in hydroxyl radical ($^{\circ}\text{OH}$)
846 generation [248]. Various methods have been tested and validated by researchers to
847 develop biochar supported catalyst for the activation of hydrogen peroxide and persulfate

848 such as; co-precipitation, impregnation, liquid phase reduction, hydrothermal and
849 pyrolysis [249][250]. Meanwhile, the role of biochar in hydroxyl radical based AOPs can
850 be classified in three categories; biochar as a catalyst, biochar as supporting material and
851 biochar as cathode in electro-Fenton process [251].

852 Some works reported the synthesis of biochar composite with a double function of
853 adsorption and photocatalytic degradation. Leichtweis et al., reported the preparation of
854 biochar derived from pecan nutshell with ZnO (biochar-ZnO) for the treatment of acid red
855 97 in aqueous solution. The obtained material degraded 100% of acid red 97 in only 67
856 min of treatment (30 min with biosorption + 37 min with photocatalysis) [252]. Similar
857 results reported by Xiao et al., on the treatment of enrofloxacin with 50% g-C₃N₄/biochar,
858 report a removal of 45.2% and 81.1% of enrofloxacin (C₀=10 mg/L) under darkness and
859 light with a material dosage of 1 mg/mL, respectively [175]. It is worth mentioning that
860 about 98 % of tetracycline removal was achieved by MnFe-LDO–biochar catalyst within
861 240 min upon exposure to a UV light [174]. On the other hand, Luo et al., reviewed the
862 formation mechanisms of persistent free radicals in biochar and their interactions with
863 organic and inorganic contaminants. They reported the combination of biochar with
864 different oxidation processes such as; H₂O₂, photocatalysis, peroxydisulfate, persulfates,
865 peroxymonosulfate [9]. It is also reported that the effect of some typical anions such as;
866 SO₄²⁻, H₂PO₄⁻, HCO₃⁻ and Cl⁻ can act as inhibitors by trapping the radicals and therefore
867 compete with the adsorption [253].

868 The electrical discharge plasma was also coupled with biochar as reported by Lou et al.,
869 for the degradation of tetracycline hydrochloride in aqueous medium [254]. The result
870 showed that during discharge plasma process, the specific surface area and the amount

871 of oxygen-containing functional groups of biochar increased due to the interaction of
872 biochar and reactive species generated by the plasma. The amount of generated $\cdot\text{OH}$
873 radicals was higher in the combined system due to the decomposition of O_3 and H_2O_2 .
874 Furthermore, this process leads to the elimination of tetracycline hydrochloride ($C_0=50$
875 mg/L) at 89.36% in only 5 min [254].

876

877 **7. Water treatment by biochar at pilot scale**

878

879 Nowadays, the development of biochar based pilot or industrial plant reactors for
880 contaminated water treatment is of great importance, because of the large amount of
881 wastewater daily generated in the world [255]. There are only very few works reported on
882 the organic/inorganic pollutants removal at pilot scale biochar reactors. Ashoori et al.
883 reported the removal of nitrate, metals, and trace organic contaminants from urban
884 stormwater runoff by pilot-scale biochar-amended woodchip bioreactor, composed of 9
885 parallel columns of 10 cm in diameter and 50 cm length, where every three columns are
886 filled with the same adsorbent (Woodchips, Woodchips + biochar and Woodchips + straw).
887 The results showed a high capacity of removing nitrate and four of the five metals tested
888 (i.e., Cd, Cu, Ni and Pb but not Zn), however a weak adsorption capacity for organic
889 pollutant was recorded [256]. Finally, scientific advances on the extrapolation of results
890 present a significant challenge requiring more investigations to be conducted within the
891 framework of a reusability over several cycles.

892 **8. Conclusion and future research directions**

893

894 Biochar has been recommended as a promising adsorbent material for organic
895 contaminants removal from wastewater. Some works estimated the costs incurred in the
896 production of biochar based adsorbents; a cheaper process and a reusability ability with
897 multiple cycles of biochar is possible [85]. Nevertheless, supplementary research in
898 several perspectives is necessary to ensure the efficacy and cost-effectiveness of biochar
899 to scale-up it into a large-scale application, mostly in the following areas:

900 1) Some of the reported biochar sorbents (such as Coir pith, Coconut coir dust,
901 Pandanus leaves and paper waste) showed low efficiency and elimination capacity
902 to organic pollutants. It is expected that surface modifications will help increase their
903 capacity.

904 2) To achieve optimal environmental remediation activity for biochars it is essential to
905 further explore the relationships between certain factors; production process,
906 activation, functionalization, and treatment all in an environmental ecofriendly
907 manner.

908 3) It is important to keep in mind that a promising bio based sorbent successfully
909 applicable at industrial scale should be economically attractive and raw materials
910 should be extensively available in large quantities in nature or as a by-product (bio-
911 residues) [257]. Regenerating and reusing using these sorbents for several cycles
912 at an industrial scale can reduce the cost and energy consumption for production
913 and offer a sustainable product.

914

915 Combined modified-clay/biochar composites revealed noteworthy advantages over
916 single-modified-clays, due to their high adsorption capacity, low cost and more suitable
917 for removing anionic dyes and phenolic compounds.

918 There are a very few studies on pilot/large-scale application of biochar for organic
919 pollutants removal in literature.

920 The progress of research on magnetic biochar with catalytic degradation activity for
921 organic contaminants elimination from aqueous medium is an important and a new
922 research direction and will become a research focus soon. Studies on the toxic
923 components produced during magnetic biochar synthesis should be carefully considered.

924 The implementation of a sustainable management plan for pollutant-loaded Sewage
925 derived biochars (SDBs) is critical. This strategy should follow the circular economy
926 concept and would permit: i) an eco-friendly and low-cost regeneration and reuse of these
927 SDBs in upcoming adsorption cycles, ii) the recovery of the adsorbed chemicals and its
928 reprocess in an industry as resources, and iii) the preservation of the environment counter
929 to further pollution.

930 Two strategies concepts should be explored to achieve functional and cost-effective
931 modified biochars for the efficient elimination of organic compounds from wastewater: i)
932 The first one is optimizing the biochar physicochemical activation process using a variety
933 of eco-friendly reagents, ii) The second option concerns the exploitation of the high
934 specific surface areas of prepared biochar to impregnate nano-composites. The
935 application of an experimental design software to optimize the influencing parameter is a
936 powerful and innovative tool in the experiment design and analysis phase. Machine

937 learning (ML) is a subdivision of artificial intelligence (AI) that aims to reduce explicit
938 computers programming by learning from experience and prediction [258]. Predictive
939 models that use machine learning can reduce the workload, cost, space requirement and
940 time consumption for remediation of effluents [259]. For example ML can be applied to
941 develop prediction models for optimizing the pyrolysis process and predict biochar yield
942 and C-char according to biomass characteristics and pyrolysis conditions [260]. As stated
943 in [261], science-informed design of biochar substrates with high removal capacity for
944 organic contaminants can prove a valuable tool for designing sustainable wastewater
945 treatment systems. The developed models based on data from advanced microscopic and
946 spectroscopic techniques (biochar surface functionality and porous structure) gave
947 accurate predictions on the adsorption capacity of the considered materials.

948 The conception of more compact reactors that can accommodate biochar supported
949 catalysts are necessary for real scale applications. Future research must be devoted to
950 implement biochar-based catalysts in pilot scale reactors that can be used also at
951 industrial level.

952 Optimizing biochar properties and activation techniques and parameters is important for
953 obtaining maximum efficiency for organic pollutant elimination, less post-treatment by-
954 products and less energy consumption.

955 Well-coordinated actions currently going on, guided by the European biochar certificate
956 (EBC) in Europe, and the IBI at international level, to regulate and standardize quality
957 requirements and develop guidelines or good practices concerning the biomass supply,
958 biochar production and biochar applications which mainly are limited to agriculture and
959 organic farming. One needs to keep in mind that the first concern of the EBC has been to

960 safeguard health and safety while producing and using biochar in a sustainable way.
961 Biochar based substrates for environmental applications are a promising alternative to
962 currently applied substrates for wastewater treatment and organic pollutant elimination,
963 but there is yet no set of criteria on the physicochemical properties of the substates that
964 guarantee satisfactory adsorption efficiencies. Such well-coordinated actions are currently
965 still in the form of literature reviews that try to draw conclusions and offer a suggestions
966 and guidelines for researchers that need to build upon the existing but very dispersed
967 knowledge on the potential applications of biochar and biochar composites in
968 environmental applications.

969 **Acknowledgments**

970
971 “The authors would like to acknowledge the financial support of the INTERREG North-
972 West Europe ThreeC with the project number NWE 1010, under the umbrella of the
973 European Regional Development Fund (ERDF).”

974 **References**

- 975 [1] J.H. Park, Y.S. Ok, S.H. Kim, J.S. Cho, J.S. Heo, R.D. Delaune, D.C. Seo,
976 Competitive adsorption of heavy metals onto sesame straw biochar in aqueous
977 solutions, *Chemosphere*. 142 (2016) 77–83.
978 <https://doi.org/10.1016/j.chemosphere.2015.05.093>.
- 979 [2] P. Li, Q. Cai, W. Lin, B. Chen, B. Zhang, Offshore oil spill response practices and
980 emerging challenges, *Mar. Pollut. Bull.* 110 (2016) 6–27.
981 <https://doi.org/10.1016/j.marpolbul.2016.06.020>.
- 982 [3] F. Flesch, P. Berger, D. Robles-Vargas, G.E. Santos-Medrano, R. Rico-Martínez,
983 Characterization and determination of the toxicological risk of biochar using

- 984 invertebrate toxicity tests in the state of Aguascalientes, México, *Appl. Sci.* 9 (2019).
985 <https://doi.org/10.3390/app9081706>.
- 986 [4] R.O. Alves de Lima, A.P. Bazo, D.M.F. Salvadori, C.M. Rech, D. de Palma Oliveira,
987 G. de Aragão Umbuzeiro, Mutagenic and carcinogenic potential of a textile azo dye
988 processing plant effluent that impacts a drinking water source, *Mutat. Res. - Genet.*
989 *Toxicol. Environ. Mutagen.* 626 (2007) 53–60.
990 <https://doi.org/10.1016/j.mrgentox.2006.08.002>.
- 991 [5] H. Zeghioud, P. Nguyen-Tri, L. Khezami, A. Amrane, A.A. Assadi, Review on
992 discharge Plasma for water treatment: mechanism, reactor geometries, active
993 species and combined processes, *J. Water Process Eng.* 38 (2020) 101664.
994 <https://doi.org/10.1016/j.jwpe.2020.101664>.
- 995 [6] Z. Liu, K. Demeestere, S. Van Hulle, Comparison and performance assessment of
996 ozone-based AOPs in view of trace organic contaminants abatement in water and
997 wastewater: A review, *J. Environ. Chem. Eng.* 9 (2021) 105599.
998 <https://doi.org/10.1016/j.jece.2021.105599>.
- 999 [7] S. Kim, S.N. Nam, A. Jang, M. Jang, C.M. Park, A. Son, N. Her, J. Heo, Y. Yoon,
1000 Review of adsorption–membrane hybrid systems for water and wastewater
1001 treatment, *Chemosphere.* 286 (2022) 131916.
1002 <https://doi.org/10.1016/j.chemosphere.2021.131916>.
- 1003 [8] C. Zhao, J. Zhou, Y. Yan, L. Yang, G. Xing, H. Li, P. Wu, M. Wang, H. Zheng,
1004 Application of coagulation/flocculation in oily wastewater treatment: A review, *Sci.*
1005 *Total Environ.* 765 (2021) 142795. <https://doi.org/10.1016/j.scitotenv.2020.142795>.
- 1006 [9] K. Luo, Y. Pang, D. Wang, X. Li, L. Wang, M. Lei, Q. Huang, Q. Yang, A critical
1007 review on the application of biochar in environmental pollution remediation: Role of
1008 persistent free radicals (PFRs), *J. Environ. Sci. (China).* 108 (2021) 201–216.
1009 <https://doi.org/10.1016/j.jes.2021.02.021>.
- 1010 [10] A. Othmani, J. John, H. Rajendran, A. Mansouri, M. Sillanpää, P.
1011 Velayudhaperumal Chellam, Biochar and activated carbon derivatives of
1012 lignocellulosic fibers towards adsorptive removal of pollutants from aqueous

- 1013 systems: Critical study and future insight, *Sep. Purif. Technol.* 274 (2021) 119062.
1014 <https://doi.org/10.1016/j.seppur.2021.119062>.
- 1015 [11] A. Aboudalle, H. Djelal, L. Domergue, F. Fourcade, A. Amrane, A novel system
1016 coupling an electro-Fenton process and an advanced biological process to remove
1017 a pharmaceutical compound, metronidazole, *J. Hazard. Mater.* 415 (2021) 125705.
1018 <https://doi.org/10.1016/j.jhazmat.2021.125705>.
- 1019 [12] C. Osagie, A. Othmani, S. Ghosh, A. Malloum, Z. Kashitarash Esfahani, S. Ahmadi,
1020 Dyes adsorption from aqueous media through the nanotechnology: A review, *J.*
1021 *Mater. Res. Technol.* 14 (2021) 2195–2218.
1022 <https://doi.org/10.1016/j.jmrt.2021.07.085>.
- 1023 [13] D.L.T. Nguyen, Q.A. Binh, X.C. Nguyen, T.T. Huyen Nguyen, Q.N. Vo, T.D. Nguyen,
1024 T.C. Phuong Tran, T.A. Hang Nguyen, S.Y. Kim, T.P. Nguyen, J. Bae, I.T. Kim, Q.
1025 Van Le, Metal salt-modified biochars derived from agro-waste for effective congo
1026 red dye removal, *Environ. Res.* 200 (2021) 111492.
1027 <https://doi.org/10.1016/j.envres.2021.111492>.
- 1028 [14] B. Joseph, K. Kaetzl, F. Hensgen, B. Schäfer, M. Wachendorf, Sustainability
1029 assessment of activated carbon from residual biomass used for micropollutant
1030 removal at a full-scale wastewater treatment plant, *Environ. Res. Lett.* 15 (2020).
1031 <https://doi.org/10.1088/1748-9326/ab8330>.
- 1032 [15] Johannes Lehmann and Stephen Joseph, *Biochar for Environmental Management*,
1033 2009.
- 1034 [16] S. Mandal, B. Sarkar, N. Bolan, J. Novak, Y.S. Ok, L. Van Zwieten, B.P. Singh, M.B.
1035 Kirkham, G. Choppala, K. Spokas, R. Naidu, Designing advanced biochar products
1036 for maximizing greenhouse gas mitigation potential, *Crit. Rev. Environ. Sci.*
1037 *Technol.* 46 (2016) 1367–1401. <https://doi.org/10.1080/10643389.2016.1239975>.
- 1038 [17] P.R. Yaashikaa, P.S. Kumar, S. Varjani, A. Saravanan, A critical review on the
1039 biochar production techniques, characterization, stability and applications for
1040 circular bioeconomy, *Biotechnol. Reports.* 28 (2020) e00570.
1041 <https://doi.org/10.1016/j.btre.2020.e00570>.

- 1042 [18] X. Li, J. Zhang, B. Liu, Z. Su, A critical review on the application and recent
1043 developments of post-modified biochar in supercapacitors, *J. Clean. Prod.* 310
1044 (2021) 127428. <https://doi.org/10.1016/j.jclepro.2021.127428>.
- 1045 [19] Y. Li, H. Yu, L. Liu, H. Yu, Application of co-pyrolysis biochar for the adsorption and
1046 immobilization of heavy metals in contaminated environmental substrates, *J.*
1047 *Hazard. Mater.* 420 (2021) 126655. <https://doi.org/10.1016/j.jhazmat.2021.126655>.
- 1048 [20] K. Jeyasubramanian, B. Thangagiri, A. Sakthivel, J. Dhiveethu Raja, S.
1049 Seenivasan, P. Vallinayagam, D. Madhavan, S. Malathi Devi, B. Rathika, A
1050 complete review on biochar: Production, property, multifaceted applications,
1051 interaction mechanism and computational approach, *Fuel.* 292 (2021) 120243.
1052 <https://doi.org/10.1016/j.fuel.2021.120243>.
- 1053 [21] M. Guo, W. Song, J. Tian, Biochar-Facilitated Soil Remediation: Mechanisms and
1054 Efficacy Variations, *Front. Environ. Sci.* 8 (2020).
1055 <https://doi.org/10.3389/fenvs.2020.521512>.
- 1056 [22] G.S. Ghodake, S.K. Shinde, A.A. Kadam, R.G. Saratale, G.D. Saratale, M. Kumar,
1057 R.R. Palem, H.A. AL-Shwaiman, A.M. Elgorban, A. Syed, D.Y. Kim, Review on
1058 biomass feedstocks, pyrolysis mechanism and physicochemical properties of
1059 biochar: State-of-the-art framework to speed up vision of circular bioeconomy, *J.*
1060 *Clean. Prod.* 297 (2021) 126645. <https://doi.org/10.1016/j.jclepro.2021.126645>.
- 1061 [23] S. Pang, Advances in thermochemical conversion of woody biomass to energy,
1062 fuels and chemicals, *Biotechnol. Adv.* 37 (2019) 589–597.
1063 <https://doi.org/10.1016/j.biotechadv.2018.11.004>.
- 1064 [24] Y. Li, B. Xing, Y. Ding, X. Han, S. Wang, A critical review of the production and
1065 advanced utilization of biochar via selective pyrolysis of lignocellulosic biomass,
1066 *Bioresour. Technol.* 312 (2020) 123614.
1067 <https://doi.org/10.1016/j.biortech.2020.123614>.
- 1068 [25] A. Tomczyk, Z. Sokołowska, P. Boguta, Biochar physicochemical properties:
1069 pyrolysis temperature and feedstock kind effects, *Rev. Environ. Sci. Biotechnol.* 19
1070 (2020) 191–215. <https://doi.org/10.1007/s11157-020-09523-3>.

- 1071 [26] J. Shin, U. Von Gunten, D.A. Reckhow, S. Allard, Y. Lee, Reactions of Ferrate(VI)
1072 with Iodide and Hypoiodous Acid: Kinetics, Pathways, and Implications for the Fate
1073 of Iodine during Water Treatment, *Environ. Sci. Technol.* 52 (2018) 7458–7467.
1074 <https://doi.org/10.1021/acs.est.8b01565>.
- 1075 [27] Z. Abbas, S. Ali, M. Rizwan, I.E. Zaheer, A. Malik, M.A. Riaz, M.R. Shahid, M.Z. ur
1076 Rehman, M.I. Al-Wabel, A critical review of mechanisms involved in the adsorption
1077 of organic and inorganic contaminants through biochar, *Arab. J. Geosci.* 11 (2018).
1078 <https://doi.org/10.1007/s12517-018-3790-1>.
- 1079 [28] X. Wang, Z. Guo, Z. Hu, J. Zhang, Recent advances in biochar application for water
1080 and wastewater treatment: a review, *PeerJ.* 8 (2020) e9164.
1081 <https://doi.org/10.7717/peerj.9164>.
- 1082 [29] S. Patel, S. Kundu, P. Halder, N. Ratnayake, M.H. Marzbali, S. Aktar, E.
1083 Selezneva, J. Paz-Ferreiro, A. Surapaneni, C.C. de Figueiredo, A. Sharma, M.
1084 Megharaj, K. Shah, A critical literature review on biosolids to biochar: an alternative
1085 biosolids management option, 2020. <https://doi.org/10.1007/s11157-020-09553-x>.
- 1086 [30] S. Jeffery, F.G.A. Verheijen, M. van der Velde, A.C. Bastos, A quantitative review
1087 of the effects of biochar application to soils on crop productivity using meta-analysis,
1088 *Agric. Ecosyst. Environ.* 144 (2011) 175–187.
1089 <https://doi.org/10.1016/j.agee.2011.08.015>.
- 1090 [31] K.A. Spokas, K.B. Cantrell, J.M. Novak, D.W. Archer, J.A. Ippolito, H.P. Collins, A.A.
1091 Boateng, I.M. Lima, M.C. Lamb, A.J. McAloon, R.D. Lentz, K.A. Nichols, Biochar: A
1092 Synthesis of Its Agronomic Impact beyond Carbon Sequestration, *J. Environ. Qual.*
1093 41 (2012) 973–989. <https://doi.org/10.2134/jeq2011.0069>.
- 1094 [32] Y. Zhou, S. Qin, S. Verma, T. Sar, S. Sarsaiya, B. Ravindran, T. Liu, R. Sindhu,
1095 A.K. Patel, P. Binod, S. Varjani, R. Rani Singhnia, Z. Zhang, M.K. Awasthi,
1096 Production and beneficial impact of biochar for environmental application: A
1097 comprehensive review, *Bioresour. Technol.* 337 (2021) 125451.
1098 <https://doi.org/10.1016/j.biortech.2021.125451>.
- 1099 [33] M. Patel, R. Kumar, C.U. Pittman, D. Mohan, Ciprofloxacin and acetaminophen

- 1100 sorption onto banana peel biochars: Environmental and process parameter
1101 influences, *Environ. Res.* 201 (2021) 111218.
1102 <https://doi.org/10.1016/j.envres.2021.111218>.
- 1103 [34] S.S. Mayakaduwa, P. Kumarathilaka, I. Herath, M. Ahmad, M. Al-Wabel, Y.S. Ok,
1104 A. Usman, A. Abduljabbar, M. Vithanage, Equilibrium and kinetic mechanisms of
1105 woody biochar on aqueous glyphosate removal, *Chemosphere*. 144 (2016) 2516–
1106 2521. <https://doi.org/10.1016/j.chemosphere.2015.07.080>.
- 1107 [35] M. Askeland, B. Clarke, J. Paz-Ferreiro, Comparative characterization of biochars
1108 produced at three selected pyrolysis temperatures from common woody and
1109 herbaceous waste streams, *PeerJ*. 7 (2019) 1–20.
1110 <https://doi.org/10.7717/peerj.6784>.
- 1111 [36] Q. Meng, Y. Zhang, D. Meng, X. Liu, Z. Zhang, P. Gao, A. Lin, L. Hou, Removal of
1112 sulfadiazine from aqueous solution by in-situ activated biochar derived from cotton
1113 shell, *Environ. Res.* 191 (2020) 110104.
1114 <https://doi.org/10.1016/j.envres.2020.110104>.
- 1115 [37] K. Jindo, H. Mizumoto, Y. Sawada, M.A. Sanchez-Monedero, T. Sonoki, Physical
1116 and chemical characterization of biochars derived from different agricultural
1117 residues, *Biogeosciences*. 11 (2014) 6613–6621. [https://doi.org/10.5194/bg-11-](https://doi.org/10.5194/bg-11-6613-2014)
1118 [6613-2014](https://doi.org/10.5194/bg-11-6613-2014).
- 1119 [38] B. Hu, Y. Tang, X. Wang, L. Wu, J. Nong, X. Yang, J. Guo, Cobalt-gadolinium
1120 modified biochar as an adsorbent for antibiotics in single and binary systems,
1121 *Microchem. J.* 166 (2021) 106235. <https://doi.org/10.1016/j.microc.2021.106235>.
- 1122 [39] Y. Liu, F. Li, J. Deng, Z. Wu, T. Lei, M. Tan, Z. Wu, X. Qin, H. Li, Mechanism of
1123 sulfamic acid modified biochar for highly efficient removal of tetracycline, *J. Anal.*
1124 *Appl. Pyrolysis*. 158 (2021) 105247. <https://doi.org/10.1016/j.jaap.2021.105247>.
- 1125 [40] J. Li, Y. Liu, X. Ren, W. Dong, H. Chen, T. Cai, W. Zeng, W. Li, L. Tang, Soybean
1126 residue based biochar prepared by ball milling assisted alkali activation to activate
1127 peroxydisulfate for the degradation of tetracycline, *J. Colloid Interface Sci.* 599
1128 (2021) 631–641. <https://doi.org/10.1016/j.jcis.2021.04.074>.

- 1129 [41] T. Chen, L. Luo, S. Deng, G. Shi, S. Zhang, Y. Zhang, O. Deng, L. Wang, J. Zhang,
1130 L. Wei, Sorption of tetracycline on H₃PO₄ modified biochar derived from rice straw
1131 and swine manure, *Bioresour. Technol.* 267 (2018) 431–437.
1132 <https://doi.org/10.1016/j.biortech.2018.07.074>.
- 1133 [42] V. Singh, V.C. Srivastava, Self-engineered iron oxide nanoparticle incorporated on
1134 mesoporous biochar derived from textile mill sludge for the removal of an emerging
1135 pharmaceutical pollutant, *Environ. Pollut.* 259 (2020) 113822.
1136 <https://doi.org/10.1016/j.envpol.2019.113822>.
- 1137 [43] M.B. Ahmed, J.L. Zhou, H.H. Ngo, W. Guo, M.A.H. Jahir, K. Sornalingam, Single
1138 and competitive sorption properties and mechanism of functionalized biochar for
1139 removing sulfonamide antibiotics from water, *Chem. Eng. J.* 311 (2017) 348–358.
1140 <https://doi.org/10.1016/j.cej.2016.11.106>.
- 1141 [44] Z. Shirani, H. Song, A. Bhatnagar, Efficient removal of diclofenac and cephalexin
1142 from aqueous solution using *Anthriscus sylvestris*-derived activated biochar, *Sci.*
1143 *Total Environ.* 745 (2020) 140789. <https://doi.org/10.1016/j.scitotenv.2020.140789>.
- 1144 [45] Y. Zhang, R. Fan, Q. Zhang, Y. Chen, O. Sharifi, D. Leszczynska, R. Zhang, Q. Dai,
1145 Synthesis of CaWO₄-biochar nanocomposites for organic dye removal, *Mater. Res.*
1146 *Bull.* 110 (2019) 169–173. <https://doi.org/10.1016/j.materresbull.2018.10.031>.
- 1147 [46] F. Yu, F. Tian, H. Zou, Z. Ye, C. Peng, J. Huang, Y. Zheng, Y. Zhang, Y. Yang, X.
1148 Wei, B. Gao, ZnO/biochar nanocomposites via solvent free ball milling for enhanced
1149 adsorption and photocatalytic degradation of methylene blue, *J. Hazard. Mater.* 415
1150 (2021) 125511. <https://doi.org/10.1016/j.jhazmat.2021.125511>.
- 1151 [47] X. Li, Y. Jia, M. Zhou, X. Su, J. Sun, High-efficiency degradation of organic
1152 pollutants with Fe, N co-doped biochar catalysts via persulfate activation, *J. Hazard.*
1153 *Mater.* 397 (2020) 122764. <https://doi.org/10.1016/j.jhazmat.2020.122764>.
- 1154 [48] R. Gurav, S.K. Bhatia, T.-R. Choi, H.J. Kim, Y.-K. Choi, H.-J. Lee, S. Ham, J.Y. Cho,
1155 S.H. Kim, S.H. Lee, J. Yun, Y.-H. Yang, Adsorptive removal of synthetic plastic
1156 components bisphenol-A and solvent black-3 dye from single and binary solutions
1157 using pristine pinecone biochar, *Chemosphere.* 296 (2022) 134034.

- 1158 <https://doi.org/10.1016/j.chemosphere.2022.134034>.
- 1159 [49] F. Suo, X. You, Y. Ma, Y. Li, Rapid removal of triazine pesticides by P doped biochar
1160 and the adsorption mechanism, *Chemosphere*. 235 (2019) 918–925.
1161 <https://doi.org/10.1016/j.chemosphere.2019.06.158>.
- 1162 [50] S. Xiong, Y. Deng, R. Tang, C. Zhang, J. Zheng, Y. Zhang, L. Su, L. Yang, C. Liao,
1163 D. Gong, Factors study for the removal of epoxiconazole in water by common
1164 biochars, *Biochem. Eng. J.* 161 (2020) 107690.
1165 <https://doi.org/10.1016/j.bej.2020.107690>.
- 1166 [51] J.Y. Yoon, J.E. Kim, H.J. Song, K. Bin Oh, J.W. Jo, Y.H. Yang, S.H. Lee, G. Kang,
1167 H.J. Kim, Y.K. Choi, Assessment of adsorptive behaviors and properties of grape
1168 pomace-derived biochar as adsorbent for removal of cymoxanil pesticide, *Environ.*
1169 *Technol. Innov.* 21 (2021) 101242. <https://doi.org/10.1016/j.eti.2020.101242>.
- 1170 [52] C. Sun, T. Chen, Q. Huang, M. Zhan, X. Li, J. Yan, Activation of persulfate by CO₂-
1171 activated biochar for improved phenolic pollutant degradation: Performance and
1172 mechanism, *Chem. Eng. J.* 380 (2020) 122519.
1173 <https://doi.org/10.1016/j.cej.2019.122519>.
- 1174 [53] Y. Ma, Y. Qi, T. Lu, L. Yang, L. Wu, S. Cui, Y. Ding, Z. Zhang, Highly efficient
1175 removal of imidacloprid using potassium hydroxide activated magnetic microporous
1176 loofah sponge biochar, *Sci. Total Environ.* 765 (2021).
1177 <https://doi.org/10.1016/j.scitotenv.2020.144253>.
- 1178 [54] S. Liu, M. Li, Y. Liu, N. Liu, X. Tan, L. Jiang, J. Wen, X. Hu, Z. Yin, Removal of 17 β -
1179 estradiol from aqueous solution by graphene oxide supported activated magnetic
1180 biochar: Adsorption behavior and mechanism, *J. Taiwan Inst. Chem. Eng.* 102
1181 (2019) 330–339. <https://doi.org/10.1016/j.jtice.2019.05.002>.
- 1182 [55] J. Ding, W. Xu, S. Liu, Y. Liu, X. Tan, X. Li, Z. Li, P. Zhang, L. Du, M. Li, Activation
1183 of persulfate by nanoscale zero-valent iron loaded porous graphitized biochar for
1184 the removal of 17 β -estradiol: Synthesis, performance and mechanism, *J. Colloid*
1185 *Interface Sci.* 588 (2021) 776–786. <https://doi.org/10.1016/j.jcis.2020.11.111>.

- 1186 [56] S. Cai, Q. Zhang, Z. Wang, S. Hua, D. Ding, T. Cai, R. Zhang, Pyrrolic N-rich biochar
1187 without exogenous nitrogen doping as a functional material for bisphenol A removal:
1188 Performance and mechanism, *Appl. Catal. B Environ.* 291 (2021) 120093.
1189 <https://doi.org/10.1016/j.apcatb.2021.120093>.
- 1190 [57] L. Xiang, S. Liu, S. Ye, H. Yang, B. Song, F. Qin, M. Shen, C. Tan, G. Zeng, X. Tan,
1191 Potential hazards of biochar: The negative environmental impacts of biochar
1192 applications, *J. Hazard. Mater.* 420 (2021) 126611.
1193 <https://doi.org/10.1016/j.jhazmat.2021.126611>.
- 1194 [58] X. Ma, B. Zhou, A. Budai, A. Jeng, X. Hao, D. Wei, Y. Zhang, D. Rasse, Study of
1195 Biochar Properties by Scanning Electron Microscope – Energy Dispersive X-Ray
1196 Spectroscopy (SEM-EDX), *Commun. Soil Sci. Plant Anal.* 47 (2016) 593–601.
1197 <https://doi.org/10.1080/00103624.2016.1146742>.
- 1198 [59] L. Wang, Surface Properties and Chemical Composition of Corncob and
1199 Miscanthus Biochars : Effects of Production Temperature Surface Properties and
1200 Chemical Composition of Corncob and Miscanthus Biochars : Effects of Production
1201 Temperature and Method, (2017).
- 1202 [60] K. Wiedner, C. Naisse, C. Rumpel, A. Pozzi, P. Wiczecek, B. Glaser, Chemical
1203 modification of biomass residues during hydrothermal carbonization - What makes
1204 the difference, temperature or feedstock?, *Org. Geochem.* 54 (2013) 91–100.
1205 <https://doi.org/10.1016/j.orggeochem.2012.10.006>.
- 1206 [61] J.W. Lee, M. Kidder, B.R. Evans, S. Paik, A.C. Buchanan, C.T. Garten, R.C. Brown,
1207 Characterization of biochars produced from cornstovers for soil amendment,
1208 *Environ. Sci. Technol.* 44 (2010) 7970–7974. <https://doi.org/10.1021/es101337x>.
- 1209 [62] B. Chen, D. Zhou, L. Zhu, Transitional adsorption and partition of nonpolar and polar
1210 aromatic contaminants by biochars of pine needles with different pyrolytic
1211 temperatures, *Environ. Sci. Technol.* 42 (2008) 5137–5143.
1212 <https://doi.org/10.1021/es8002684>.
- 1213 [63] Y. Chun, G. Sheng, G.T. Chiou, B. Xing, Compositions and sorptive properties of
1214 crop residue-derived chars, *Environ. Sci. Technol.* 38 (2004) 4649–4655.

- 1215 <https://doi.org/10.1021/es035034w>.
- 1216 [64] Q. Shen, Z. Wang, Q. Yu, Y. Cheng, Z. Liu, T. Zhang, S. Zhou, Removal of
1217 tetracycline from an aqueous solution using manganese dioxide modified biochar
1218 derived from Chinese herbal medicine residues, *Environ. Res.* 183 (2020) 109195.
1219 <https://doi.org/10.1016/j.envres.2020.109195>.
- 1220 [65] G.C. Smith, Spectroscopy Analysis of Biochar, *Biochar A Guid. to Anal. Methods.*
1221 (2019).
- 1222 [66] P. Zhang, D. O'Connor, Y. Wang, L. Jiang, T. Xia, L. Wang, D.C.W. Tsang, Y.S.
1223 Ok, D. Hou, A green biochar/iron oxide composite for methylene blue removal, *J.*
1224 *Hazard. Mater.* 384 (2020) 121286. <https://doi.org/10.1016/j.jhazmat.2019.121286>.
- 1225 [67] Z. yang Zhang, X. cheng Xu, Wrapping carbon nanotubes with poly (sodium 4-
1226 styrenesulfonate) for enhanced adsorption of methylene blue and its mechanism,
1227 *Chem. Eng. J.* 256 (2014) 85–92. <https://doi.org/10.1016/j.cej.2014.06.020>.
- 1228 [68] J. Iqbal, N.S. Shah, M. Sayed, N.K. Niazi, M. Imran, J.A. Khan, Z.U.H. Khan, A.G.S.
1229 Hussien, K. Polychronopoulou, F. Howari, Nano-zerovalent manganese/biochar
1230 composite for the adsorptive and oxidative removal of Congo-red dye from aqueous
1231 solutions, *J. Hazard. Mater.* 403 (2021) 123854.
1232 <https://doi.org/10.1016/j.jhazmat.2020.123854>.
- 1233 [69] N. Zhao, K. Liu, B. Yan, L. Zhu, C. Zhao, J. Gao, J. Ruan, W. Zhang, R. Qiu,
1234 Chlortetracycline hydrochloride removal by different biochar/Fe composites: A
1235 comparative study, *J. Hazard. Mater.* 403 (2021) 123889.
1236 <https://doi.org/10.1016/j.jhazmat.2020.123889>.
- 1237 [70] Y. Ma, L. Wu, P. Li, L. Yang, L. He, S. Chen, Y. Yang, F. Gao, X. Qi, Z. Zhang, A
1238 novel, efficient and sustainable magnetic sludge biochar modified by graphene
1239 oxide for environmental concentration imidacloprid removal, *J. Hazard. Mater.* 407
1240 (2021). <https://doi.org/10.1016/j.jhazmat.2020.124777>.
- 1241 [71] H. Cheng, Y. Liu, X. Li, Adsorption performance and mechanism of iron-loaded
1242 biochar to methyl orange in the presence of Cr⁶⁺ from dye wastewater, *J. Hazard.*

- 1243 Mater. 415 (2021) 125749. <https://doi.org/10.1016/j.jhazmat.2021.125749>.
- 1244 [72] F.X. Dong, L. Yan, X.H. Zhou, S.T. Huang, J.Y. Liang, W.X. Zhang, Z.W. Guo, P.R.
1245 Guo, W. Qian, L.J. Kong, W. Chu, Z.H. Diao, Simultaneous adsorption of Cr(VI) and
1246 phenol by biochar-based iron oxide composites in water: Performance, kinetics and
1247 mechanism, J. Hazard. Mater. 416 (2021) 125930.
1248 <https://doi.org/10.1016/j.jhazmat.2021.125930>.
- 1249 [73] X. Bai, Y. Zhang, J. Shi, L. Xu, Y. Wang, P. Jin, A new application pattern for sludge-
1250 derived biochar adsorbent: Ideal persulfate activator for the high-efficiency
1251 mineralization of pollutants, J. Hazard. Mater. 419 (2021).
1252 <https://doi.org/10.1016/j.jhazmat.2021.126343>.
- 1253 [74] X. Chen, H. Li, W. Liu, Z. Meng, Z. Wu, G. Wang, Y. Liang, S. Bi, Low-temperature
1254 constructing N-doped graphite-like mesoporous structure biochar from furfural
1255 residue with urea for removal of chlortetracycline from wastewater and hydrothermal
1256 catalytic degradation mechanism, Colloids Surfaces A Physicochem. Eng. Asp. 600
1257 (2020) 124873. <https://doi.org/10.1016/j.colsurfa.2020.124873>.
- 1258 [75] Y. Ma, M. Li, P. Li, L. Yang, L. Wu, F. Gao, X. Qi, Z. Zhang, Hydrothermal synthesis
1259 of magnetic sludge biochar for tetracycline and ciprofloxacin adsorptive removal,
1260 Bioresour. Technol. 319 (2021). <https://doi.org/10.1016/j.biortech.2020.124199>.
- 1261 [76] X. Zheng, X. He, H. Peng, J. Wen, S. Lv, Efficient adsorption of ciprofloxacin using
1262 Ga₂S₃/S-modified biochar via the high-temperature sulfurization, Bioresour.
1263 Technol. 334 (2021) 125238. <https://doi.org/10.1016/j.biortech.2021.125238>.
- 1264 [77] Y. Zhang, Y. Zheng, Y. Yang, J. Huang, A.R. Zimmerman, H. Chen, X. Hu, B. Gao,
1265 Mechanisms and adsorption capacities of hydrogen peroxide modified ball milled
1266 biochar for the removal of methylene blue from aqueous solutions, Bioresour.
1267 Technol. 337 (2021) 125432. <https://doi.org/10.1016/j.biortech.2021.125432>.
- 1268 [78] K.A. Spokas, Review of the stability of biochar in soils: Predictability of O:C molar
1269 ratios, Carbon Manag. 1 (2010) 289–303. <https://doi.org/10.4155/cmt.10.32>.
- 1270 [79] M.I. Al-Wabel, M. Ahmad, A.R.A. Usman, A.S.F. Al-Farraj, Designing chitosan

- 1271 based magnetic beads with conocarpus waste-derived biochar for efficient
1272 sulfathiazole removal from contaminated water, Saudi J. Biol. Sci. (2021).
1273 <https://doi.org/10.1016/j.sjbs.2021.06.072>.
- 1274 [80] C.H. Chia, B. Gong, S.D. Joseph, C.E. Marjo, P. Munroe, A.M. Rich, Imaging of
1275 mineral-enriched biochar by FTIR, Raman and SEM-EDX, Vib. Spectrosc. 62
1276 (2012) 248–257. <https://doi.org/10.1016/j.vibspec.2012.06.006>.
- 1277 [81] Y. Luo, M. Durenkamp, M. De Nobili, Q. Lin, B.J. Devonshire, P.C. Brookes,
1278 Microbial biomass growth, following incorporation of biochars produced at 350 °C
1279 or 700 °C, in a silty-clay loam soil of high and low pH, Soil Biol. Biochem. 57 (2013)
1280 513–523. <https://doi.org/10.1016/j.soilbio.2012.10.033>.
- 1281 [82] J. Shin, Y.G. Lee, S.H. Lee, S. Kim, D. Ochir, Y. Park, J. Kim, K. Chon, Single and
1282 competitive adsorptions of micropollutants using pristine and alkali-modified
1283 biochars from spent coffee grounds, J. Hazard. Mater. 400 (2020) 123102.
1284 <https://doi.org/10.1016/j.jhazmat.2020.123102>.
- 1285 [83] G. Prasannamedha, P.S. Kumar, R. Mehala, T.J. Sharumitha, D. Surendhar,
1286 Enhanced adsorptive removal of sulfamethoxazole from water using biochar
1287 derived from hydrothermal carbonization of sugarcane bagasse, J. Hazard. Mater.
1288 407 (2021) 124825. <https://doi.org/10.1016/j.jhazmat.2020.124825>.
- 1289 [84] Z. Wen, J. Xi, J. Lu, Y. Zhang, G. Cheng, Y. Zhang, R. Chen, Porous biochar-
1290 supported MnFe₂O₄ magnetic nanocomposite as an excellent adsorbent for
1291 simultaneous and effective removal of organic/inorganic arsenic from water, J.
1292 Hazard. Mater. 411 (2021) 124909. <https://doi.org/10.1016/j.jhazmat.2020.124909>.
- 1293 [85] P. Chakraborty, S. Show, S. Banerjee, G. Halder, Mechanistic insight into sorptive
1294 elimination of ibuprofen employing bi-directional activated biochar from sugarcane
1295 bagasse: Performance evaluation and cost estimation, J. Environ. Chem. Eng. 6
1296 (2018) 5287–5300. <https://doi.org/10.1016/j.jece.2018.08.017>.
- 1297 [86] X. Yang, X. Zhang, Z. Wang, S. Li, J. Zhao, G. Liang, X. Xie, Mechanistic insights
1298 into removal of norfloxacin from water using different natural iron ore – biochar
1299 composites: more rich free radicals derived from natural pyrite-biochar composites

- 1300 than hematite-biochar composites, *Appl. Catal. B Environ.* 255 (2019) 117752.
1301 <https://doi.org/10.1016/j.apcatb.2019.117752>.
- 1302 [87] Y. Gu, Y. Xue, D. Zhang, Preparation of magnetic biochar with different
1303 magnetization sequences for efficient removal of oxytetracycline from aqueous
1304 solution, *Colloids Surfaces A Physicochem. Eng. Asp.* 626 (2021).
1305 <https://doi.org/10.1016/j.colsurfa.2021.126987>.
- 1306 [88] A.A. Lawal, M.A. Hassan, M.A.A. Farid, T.A.T. Yasim-Anuar, M.Z.M. Yusoff, M.R.
1307 Zakaria, A.M. Roslan, M.N. Mokhtar, Y. Shirai, Production of biochar from oil palm
1308 frond by steam pyrolysis for removal of residual contaminants in palm oil mill effluent
1309 final discharge, *J. Clean. Prod.* 265 (2020) 121643.
1310 <https://doi.org/10.1016/j.jclepro.2020.121643>.
- 1311 [89] R. Singh, D. V. Naik, R.K. Dutta, P.K. Kanaujia, Biochars for the removal of
1312 naphthenic acids from water: A prospective approach towards remediation of
1313 petroleum refinery wastewater, *J. Clean. Prod.* 266 (2020) 121986.
1314 <https://doi.org/10.1016/j.jclepro.2020.121986>.
- 1315 [90] Y. Wang, H. Dong, L. Li, R. Tian, J. Chen, Q. Ning, B. Wang, L. Tang, G. Zeng,
1316 Influence of feedstocks and modification methods on biochar's capacity to activate
1317 hydrogen peroxide for tetracycline removal, *Bioresour. Technol.* 291 (2019) 121840.
1318 <https://doi.org/10.1016/j.biortech.2019.121840>.
- 1319 [91] M.J. Fernandes, M.M. Moreira, P. Paíga, D. Dias, M. Bernardo, M. Carvalho, N.
1320 Lapa, I. Fonseca, S. Morais, S. Figueiredo, C. Delerue-Matos, Evaluation of the
1321 adsorption potential of biochars prepared from forest and agri-food wastes for the
1322 removal of fluoxetine, *Bioresour. Technol.* 292 (2019) 121973.
1323 <https://doi.org/10.1016/j.biortech.2019.121973>.
- 1324 [92] H. Wang, S. Wang, Y. Gao, Cetyl trimethyl ammonium bromide modified magnetic
1325 biochar from pine nut shells for efficient removal of acid chrome blue K, *Bioresour.*
1326 *Technol.* 312 (2020) 123564. <https://doi.org/10.1016/j.biortech.2020.123564>.
- 1327 [93] Z. Zhang, Y. Li, L. Ding, J. Yu, Q. Zhou, Y. Kong, J. Ma, Novel sodium bicarbonate
1328 activation of cassava ethanol sludge derived biochar for removing tetracycline from

- 1329 aqueous solution: Performance assessment and mechanism insight, *Bioresour.*
1330 *Technol.* 330 (2021) 124949. <https://doi.org/10.1016/j.biortech.2021.124949>.
- 1331 [94] E.T. Yun, J.H. Lee, J. Kim, H.D. Park, J. Lee, Identifying the Nonradical Mechanism
1332 in the Peroxymonosulfate Activation Process: Singlet Oxygenation Versus Mediated
1333 Electron Transfer, *Environ. Sci. Technol.* 52 (2018) 7032–7042.
1334 <https://doi.org/10.1021/acs.est.8b00959>.
- 1335 [95] X. Rong, M. Xie, L. Kong, V. Natarajan, L. Ma, J. Zhan, The magnetic biochar
1336 derived from banana peels as a persulfate activator for organic contaminants
1337 degradation, *Chem. Eng. J.* 372 (2019) 294–303.
1338 <https://doi.org/10.1016/j.cej.2019.04.135>.
- 1339 [96] D. Ouyang, Y. Chen, J. Yan, L. Qian, L. Han, M. Chen, Activation mechanism of
1340 peroxy-monosulfate by biochar for catalytic degradation of 1,4-dioxane: Important
1341 role of biochar defect structures, *Chem. Eng. J.* 370 (2019) 614–624.
1342 <https://doi.org/10.1016/j.cej.2019.03.235>.
- 1343 [97] L. Yang, Y. Chen, D. Ouyang, J. Yan, L. Qian, L. Han, M. Chen, J. Li, M. Gu,
1344 Mechanistic insights into adsorptive and oxidative removal of monochlorobenzene
1345 in biochar-supported nanoscale zero-valent iron/persulfate system, *Chem. Eng. J.*
1346 400 (2020) 125811. <https://doi.org/10.1016/j.cej.2020.125811>.
- 1347 [98] Y. Hou, Y. Liang, H. Hu, Y. Tao, J. Zhou, J. Cai, Facile preparation of multi-porous
1348 biochar from lotus biomass for methyl orange removal: Kinetics, isotherms, and
1349 regeneration studies, *Bioresour. Technol.* 329 (2021) 124877.
1350 <https://doi.org/10.1016/j.biortech.2021.124877>.
- 1351 [99] Y. Sun, I.K.M. Yu, D.C.W. Tsang, J. Fan, J.H. Clark, G. Luo, S. Zhang, E. Khan,
1352 N.J.D. Graham, Tailored design of graphitic biochar for high-efficiency and
1353 chemical-free microwave-assisted removal of refractory organic contaminants,
1354 *Chem. Eng. J.* 398 (2020) 125505. <https://doi.org/10.1016/j.cej.2020.125505>.
- 1355 [100] J.C. Lee, H.J. Kim, H.W. Kim, H. Lim, Iron-impregnated spent coffee ground biochar
1356 for enhanced degradation of methylene blue during cold plasma application, *J. Ind.*
1357 *Eng. Chem.* 98 (2021) 383–388. <https://doi.org/10.1016/j.jiec.2021.03.026>.

- 1358 [101] J.E. Kim, S.K. Bhatia, H.J. Song, E. Yoo, H.J. Jeon, J.Y. Yoon, Y. Yang, R. Gurav,
1359 Y.H. Yang, H.J. Kim, Y.K. Choi, Adsorptive removal of tetracycline from aqueous
1360 solution by maple leaf-derived biochar, *Bioresour. Technol.* 306 (2020) 123092.
1361 <https://doi.org/10.1016/j.biortech.2020.123092>.
- 1362 [102] J. Zhang, W. Lu, S. Zhan, J. Qiu, X. Wang, Z. Wu, H. Li, Z. Qiu, H. Peng, Adsorption
1363 and mechanistic study for humic acid removal by magnetic biochar derived from
1364 forestry wastes functionalized with Mg/Al-LDH, *Sep. Purif. Technol.* 276 (2021)
1365 119296. <https://doi.org/10.1016/j.seppur.2021.119296>.
- 1366 [103] S. Deng, J. Chen, J. Chang, Application of biochar as an innovative substrate in
1367 constructed wetlands/biofilters for wastewater treatment: Performance and
1368 ecological benefits, *J. Clean. Prod.* 293 (2021) 126156.
1369 <https://doi.org/10.1016/j.jclepro.2021.126156>.
- 1370 [104] H. Lyu, Y. He, J. Tang, M. Hecker, Q. Liu, P.D. Jones, G. Codling, J.P. Giesy, Effect
1371 of pyrolysis temperature on potential toxicity of biochar if applied to the environment,
1372 *Environ. Pollut.* 218 (2016) 1–7. <https://doi.org/10.1016/j.envpol.2016.08.014>.
- 1373 [105] P. Oleszczuk, I. Joško, M. Kuśmierz, Biochar properties regarding to contaminants
1374 content and ecotoxicological assessment, *J. Hazard. Mater.* 260 (2013) 375–382.
1375 <https://doi.org/10.1016/j.jhazmat.2013.05.044>.
- 1376 [106] G. Visioli, F.D. Conti, C. Menta, M. Bandiera, A. Malcevschi, D.L. Jones, T.
1377 Vamerali, Assessing biochar ecotoxicology for soil amendment by root phytotoxicity
1378 bioassays, *Environ. Monit. Assess.* 188 (2016) 1–11.
1379 <https://doi.org/10.1007/s10661-016-5173-y>.
- 1380 [107] S.E. Hale, J. Lehmann, D. Rutherford, A.R. Zimmerman, R.T. Bachmann, V.
1381 Shitumbanuma, A. O'Toole, K.L. Sundqvist, H.P.H. Arp, G. Cornelissen, Quantifying
1382 the total and bioavailable polycyclic aromatic hydrocarbons and dioxins in biochars,
1383 *Environ. Sci. Technol.* 46 (2012) 2830–2838. <https://doi.org/10.1021/es203984k>.
- 1384 [108] B. Pan, H. Li, D. Lang, B. Xing, Environmentally persistent free radicals:
1385 Occurrence, formation mechanisms and implications, *Environ. Pollut.* 248 (2019)
1386 320–331. <https://doi.org/10.1016/j.envpol.2019.02.032>.

- 1387 [109] C. Zhang, G. Zeng, D. Huang, C. Lai, M. Chen, M. Cheng, W. Tang, L. Tang, H.
1388 Dong, B. Huang, X. Tan, R. Wang, Biochar for environmental management:
1389 Mitigating greenhouse gas emissions, contaminant treatment, and potential
1390 negative impacts, *Chem. Eng. J.* 373 (2019) 902–922.
1391 <https://doi.org/10.1016/j.cej.2019.05.139>.
- 1392 [110] K. von Gunten, M.S. Alam, M. Hubmann, Y.S. Ok, K.O. Konhauser, D.S. Alessi,
1393 Modified sequential extraction for biochar and petroleum coke: Metal release
1394 potential and its environmental implications, *Bioresour. Technol.* 236 (2017) 106–
1395 110. <https://doi.org/10.1016/j.biortech.2017.03.162>.
- 1396 [111] J.K.M. Chagas, C.C. de Figueiredo, J. da Silva, J. Paz-Ferreiro, The residual effect
1397 of sewage sludge biochar on soil availability and bioaccumulation of heavy metals:
1398 Evidence from a three-year field experiment, *J. Environ. Manage.* 279 (2021).
1399 <https://doi.org/10.1016/j.jenvman.2020.111824>.
- 1400 [112] P. Devi, A.K. Saroha, Risk analysis of pyrolyzed biochar made from paper mill
1401 effluent treatment plant sludge for bioavailability and eco-toxicity of heavy metals,
1402 *Bioresour. Technol.* 162 (2014) 308–315.
1403 <https://doi.org/10.1016/j.biortech.2014.03.093>.
- 1404 [113] X. Chen, L. Yang, S.C.B. Myneni, Y. Deng, Leaching of polycyclic aromatic
1405 hydrocarbons (PAHs) from sewage sludge-derived biochar, *Chem. Eng. J.* 373
1406 (2019) 840–845. <https://doi.org/10.1016/j.cej.2019.05.059>.
- 1407 [114] K. Wiedner, C. Rumpel, C. Steiner, A. Pozzi, R. Maas, B. Glaser, Chemical
1408 evaluation of chars produced by thermochemical conversion (gasification, pyrolysis
1409 and hydrothermal carbonization) of agro-industrial biomass on a commercial scale,
1410 *Biomass and Bioenergy.* 59 (2013) 264–278.
1411 <https://doi.org/10.1016/j.biombioe.2013.08.026>.
- 1412 [115] E.S. Odinga, M.G. Waigi, F.O. Gudda, J. Wang, B. Yang, X. Hu, S. Li, Y. Gao,
1413 Occurrence, formation, environmental fate and risks of environmentally persistent
1414 free radicals in biochars, *Environ. Int.* 134 (2020) 105172.
1415 <https://doi.org/10.1016/j.envint.2019.105172>.

- 1416 [116] M. Lei, S. Wu, J. Liang, C. Liu, Comprehensive understanding the chemical
1417 structure evolution and crucial intermediate radical in situ observation in enzymatic
1418 hydrolysis/mild acidolysis lignin pyrolysis, *J. Anal. Appl. Pyrolysis*. 138 (2019) 249–
1419 260. <https://doi.org/10.1016/j.jaap.2019.01.004>.
- 1420 [117] S. Liao, B. Pan, H. Li, D. Zhang, B. Xing, Detecting free radicals in biochars and
1421 determining their ability to inhibit the germination and growth of corn, wheat and rice
1422 seedlings, *Environ. Sci. Technol.* 48 (2014) 8581–8587.
1423 <https://doi.org/10.1021/es404250a>.
- 1424 [118] B. Dellinger, W.A. Pryor, R. Cueto, G.L. Squadrito, W.A. Deutsch, The role of
1425 combustion-generated radicals in the toxicity of PM_{2.5}, *Proc. Combust. Inst.* 28
1426 (2000) 2675–2681. [https://doi.org/10.1016/S0082-0784\(00\)80687-6](https://doi.org/10.1016/S0082-0784(00)80687-6).
- 1427 [119] H. Cui, D. Li, X. Liu, Y. Fan, X. Zhang, S. Zhang, J. Zhou, G. Fang, J. Zhou, Dry-
1428 wet and freeze-thaw aging activate endogenous copper and cadmium in biochar, *J.*
1429 *Clean. Prod.* 288 (2021) 125605. <https://doi.org/10.1016/j.jclepro.2020.125605>.
- 1430 [120] EBC (2012), European Biochar Certificate - Guidelines for a Sustainable Production
1431 of Biochar', *Eur. Biochar Found. (EBC)*, Arbaz, Switzerland. Version 6.1 19th June,
1432 (2015) 1–22.
- 1433 [121] S. Meyer, L. Genesio, I. Vogel, H.P. Schmidt, G. Soja, E. Someus, S. Shackley,
1434 F.G.A. Verheijen, B. Glaser, Biochar standardization and legislation harmonization,
1435 *J. Environ. Eng. Landsc. Manag.* 25 (2017) 175–191.
1436 <https://doi.org/10.3846/16486897.2016.1254640>.
- 1437 [122] S. Jellali, B. Khiari, M. Usman, H. Hamdi, Y. Charabi, M. Jeguirim, Sludge-derived
1438 biochars: A review on the influence of synthesis conditions on pollutants removal
1439 efficiency from wastewaters, *Renew. Sustain. Energy Rev.* 144 (2021) 111068.
1440 <https://doi.org/10.1016/j.rser.2021.111068>.
- 1441 [123] E. Salehi, M. Askari, M. Velashjerdi, B. Arab, Phosphoric acid-treated Spent Tea
1442 Residue Biochar for Wastewater Decoloring: Batch Adsorption Study and Process
1443 Intensification using Multivariate Data-based Optimization, *Chem. Eng. Process. -*
1444 *Process Intensif.* 158 (2020) 108170. <https://doi.org/10.1016/j.cep.2020.108170>.

- 1445 [124] K. AlAmeri, A. Giwa, L. Yousef, A. Alraeesi, H. Taher, Sorption and removal of crude
1446 oil spills from seawater using peat-derived biochar: An optimization study, *J.*
1447 *Environ. Manage.* 250 (2019) 109465.
1448 <https://doi.org/10.1016/j.jenvman.2019.109465>.
- 1449 [125] L. Du, W. Xu, S. Liu, X. Li, D. Huang, X. Tan, Y. Liu, Activation of persulfate by
1450 graphitized biochar for sulfamethoxazole removal: The roles of graphitic carbon
1451 structure and carbonyl group, *J. Colloid Interface Sci.* 577 (2020) 419–430.
1452 <https://doi.org/10.1016/j.jcis.2020.05.096>.
- 1453 [126] C. Wang, H. Wang, Y. Cao, Waste printed circuit boards as novel potential
1454 engineered catalyst for catalytic degradation of orange II, *J. Clean. Prod.* 221 (2019)
1455 234–241. <https://doi.org/10.1016/j.jclepro.2019.02.240>.
- 1456 [127] S. Vigneshwaran, P. Sirajudheen, M. Nikitha, K. Ramkumar, S. Meenakshi, Facile
1457 synthesis of sulfur-doped chitosan/biochar derived from tapioca peel for the removal
1458 of organic dyes: Isotherm, kinetics and mechanisms, *J. Mol. Liq.* 326 (2021) 115303.
1459 <https://doi.org/10.1016/j.molliq.2021.115303>.
- 1460 [128] A.A. Lawal, M.A. Hassan, M.A. Ahmad Farid, T.A. Tengku Yasim-Anuar, M.H.
1461 Samsudin, M.Z. Mohd Yusoff, M.R. Zakaria, M.N. Mokhtar, Y. Shirai, Adsorption
1462 mechanism and effectiveness of phenol and tannic acid removal by biochar
1463 produced from oil palm frond using steam pyrolysis, *Environ. Pollut.* 269 (2021).
1464 <https://doi.org/10.1016/j.envpol.2020.116197>.
- 1465 [129] G. Tan, Y. Wu, Y. Liu, D. Xiao, Removal of Pb(II) ions from aqueous solution by
1466 manganese oxide coated rice straw biochar – A low-cost and highly effective
1467 sorbent, *J. Taiwan Inst. Chem. Eng.* 84 (2018) 85–92.
1468 <https://doi.org/10.1016/j.jtice.2017.12.031>.
- 1469 [130] A. El Kassimi, A. Boutouil, M. El Himri, M. Rachid Laamari, M. El Haddad, Selective
1470 and competitive removal of three basic dyes from single, binary and ternary systems
1471 in aqueous solutions: A combined experimental and theoretical study, *J. Saudi*
1472 *Chem. Soc.* 24 (2020) 527–544. <https://doi.org/10.1016/j.jscs.2020.05.005>.
- 1473 [131] B. Wang, G. Lian, X. Lee, B. Gao, L. Li, T. Liu, X. Zhang, Y. Zheng, Phosphogypsum

- 1474 as a novel modifier for distillers grains biochar removal of phosphate from water,
1475 Chemosphere. 238 (2020) 124684.
1476 <https://doi.org/10.1016/j.chemosphere.2019.124684>.
- 1477 [132] N. Chaukura, E.C. Murimba, W. Gwenzi, Synthesis, characterisation and methyl
1478 orange adsorption capacity of ferric oxide–biochar nano-composites derived from
1479 pulp and paper sludge, *Appl. Water Sci.* 7 (2017) 2175–2186.
1480 <https://doi.org/10.1007/s13201-016-0392-5>.
- 1481 [133] C. Zhao, B. Wang, B.K.G. Theng, P. Wu, F. Liu, S. Wang, X. Lee, M. Chen, L. Li,
1482 X. Zhang, Formation and mechanisms of nano-metal oxide-biochar composites for
1483 pollutants removal: A review, *Sci. Total Environ.* 767 (2021) 145305.
1484 <https://doi.org/10.1016/j.scitotenv.2021.145305>.
- 1485 [134] Y. Zhou, J. Lu, Y. Zhou, Y. Liu, Recent advances for dyes removal using novel
1486 adsorbents: A review, *Environ. Pollut.* 252 (2019) 352–365.
1487 <https://doi.org/10.1016/j.envpol.2019.05.072>.
- 1488 [135] Y. Mu, H. Ma, NaOH-modified mesoporous biochar derived from tea residue for
1489 methylene Blue and Orange II removal, *Chem. Eng. Res. Des.* 167 (2021) 129–
1490 140. <https://doi.org/10.1016/j.cherd.2021.01.008>.
- 1491 [136] L. Lu, Y. Lin, Q. Chai, S. He, C. Yang, Removal of acenaphthene by biochar and
1492 raw biomass with coexisting heavy metal and phenanthrene, *Colloids Surfaces A
1493 Physicochem. Eng. Asp.* 558 (2018) 103–109.
1494 <https://doi.org/10.1016/j.colsurfa.2018.08.057>.
- 1495 [137] M.J. Iqbal, F. Cecil, K. Ahmad, M. Iqbal, M. Mushtaq, M.A. Naeem, T.H. Bokhari,
1496 Kinetic study of Cr(III) and Cr(VI) biosorption using rosa damascena phytomass: A
1497 rose waste biomass, *Asian J. Chem.* 25 (2013) 2099–2103.
1498 <https://doi.org/10.14233/ajchem.2013.13345>.
- 1499 [138] F. Sayin, S.T. Akar, T. Akar, From green biowaste to water treatment applications:
1500 Utilization of modified new biochar for the efficient removal of ciprofloxacin, *Sustain.
1501 Chem. Pharm.* 24 (2021) 100522. <https://doi.org/10.1016/j.scp.2021.100522>.

- 1502 [139] E.C. Nnadozie, P.A. Ajibade, Isotherm, kinetics, thermodynamics studies and
1503 effects of carbonization temperature on adsorption of Indigo Carmine (IC) dye using
1504 *C. odorata* biochar, *Chem. Data Collect.* 33 (2021) 100673.
1505 <https://doi.org/10.1016/j.cdc.2021.100673>.
- 1506 [140] Y. Wang, B. Jiang, L. Wang, Z. Feng, H. Fan, T. Sun, Hierarchically structured two-
1507 dimensional magnetic microporous biochar derived from hazelnut shell toward
1508 effective removal of p-arsanilic acid, *Appl. Surf. Sci.* 540 (2021) 148372.
1509 <https://doi.org/10.1016/j.apsusc.2020.148372>.
- 1510 [141] Z. Zhou, Y. guo Liu, S. bo Liu, H. yu Liu, G. ming Zeng, X. fei Tan, C. ping Yang, Y.
1511 Ding, Z. li Yan, X. xi Cai, Sorption performance and mechanisms of arsenic(V)
1512 removal by magnetic gelatin-modified biochar, *Chem. Eng. J.* 314 (2017) 223–231.
1513 <https://doi.org/10.1016/j.cej.2016.12.113>.
- 1514 [142] M. fang Li, Y. guo Liu, G. ming Zeng, S. bo Liu, X. jiang Hu, D. Shu, L. hua Jiang,
1515 X. fei Tan, X. xi Cai, Z. li Yan, Tetracycline absorbed onto nitrilotriacetic acid-
1516 functionalized magnetic graphene oxide: Influencing factors and uptake
1517 mechanism, *J. Colloid Interface Sci.* 485 (2017) 269–279.
1518 <https://doi.org/10.1016/j.jcis.2016.09.037>.
- 1519 [143] K.L. Yu, X.J. Lee, H.C. Ong, W.H. Chen, J.S. Chang, C.S. Lin, P.L. Show, T.C. Ling,
1520 Adsorptive removal of cationic methylene blue and anionic Congo red dyes using
1521 wet-torrefied microalgal biochar: Equilibrium, kinetic and mechanism modeling,
1522 *Environ. Pollut.* 272 (2021) 115986. <https://doi.org/10.1016/j.envpol.2020.115986>.
- 1523 [144] V.T. Trinh, T.M.P. Nguyen, H.T. Van, L.P. Hoang, T.V. Nguyen, L.T. Ha, X.H. Vu,
1524 T.T. Pham, T.N. Nguyen, N. V. Quang, X.C. Nguyen, Phosphate Adsorption by
1525 Silver Nanoparticles-Loaded Activated Carbon derived from Tea Residue, *Sci. Rep.*
1526 10 (2020) 1–13. <https://doi.org/10.1038/s41598-020-60542-0>.
- 1527 [145] K. Velusamy, S. Periyasamy, P.S. Kumar, T. Jayaraj, R. Krishnasamy, J. Sindhu,
1528 D. Sneka, B. Subhashini, D.V.N. Vo, Analysis on the removal of emerging
1529 contaminant from aqueous solution using biochar derived from soap nut seeds,
1530 *Environ. Pollut.* 287 (2021) 117632. <https://doi.org/10.1016/j.envpol.2021.117632>.

- 1531 [146] J. Li, G. Yu, L. Pan, C. Li, F. You, S. Xie, Y. Wang, J. Ma, X. Shang, Study of
1532 ciprofloxacin removal by biochar obtained from used tea leaves, *J. Environ. Sci.*
1533 (China). 73 (2018) 20–30. <https://doi.org/10.1016/j.jes.2017.12.024>.
- 1534 [147] K. Xu, C. Zhang, X. Dou, W. Ma, C. Wang, Optimizing the modification of wood
1535 waste biochar via metal oxides to remove and recover phosphate from human urine,
1536 *Environ. Geochem. Health*. 41 (2019) 1767–1776. [https://doi.org/10.1007/s10653-](https://doi.org/10.1007/s10653-017-9986-6)
1537 017-9986-6.
- 1538 [148] K.W. Jung, S.Y. Lee, Y.J. Lee, Hydrothermal synthesis of hierarchically structured
1539 birnessite-type MnO₂/biochar composites for the adsorptive removal of Cu(II) from
1540 aqueous media, *Bioresour. Technol.* 260 (2018) 204–212.
1541 <https://doi.org/10.1016/j.biortech.2018.03.125>.
- 1542 [149] L. Liu, G. Deng, X. Shi, Adsorption characteristics and mechanism of p-nitrophenol
1543 by pine sawdust biochar samples produced at different pyrolysis temperatures, *Sci.*
1544 *Rep.* 10 (2020) 1–11. <https://doi.org/10.1038/s41598-020-62059-y>.
- 1545 [150] L. Lonappan, T. Rouissi, S. Kaur Brar, M. Verma, R.Y. Surampalli, An insight into
1546 the adsorption of diclofenac on different biochars: Mechanisms, surface chemistry,
1547 and thermodynamics, *Bioresour. Technol.* 249 (2018) 386–394.
1548 <https://doi.org/10.1016/j.biortech.2017.10.039>.
- 1549 [151] C. Wang, H. Tan, H. Liu, B. Wu, F. Xu, H. Xu, A nanoscale ferroferric oxide coated
1550 biochar derived from mushroom waste to rapidly remove Cr(VI) and mechanism
1551 study, *Bioresour. Technol. Reports*. 7 (2019) 100253.
1552 <https://doi.org/10.1016/j.biteb.2019.100253>.
- 1553 [152] Y. Zhu, W. Dai, K. Deng, T. Pan, Z. Guan, Efficient Removal of Cr(VI) from Aqueous
1554 Solution by Fe-Mn Oxide-Modified Biochar, *Water. Air. Soil Pollut.* 231 (2020).
1555 <https://doi.org/10.1007/s11270-020-4432-2>.
- 1556 [153] Z. Wang, L. Han, K. Sun, J. Jin, K.S. Ro, J.A. Libra, X. Liu, B. Xing, Sorption of four
1557 hydrophobic organic contaminants by biochars derived from maize straw, wood dust
1558 and swine manure at different pyrolytic temperatures, *Chemosphere*. 144 (2016)
1559 285–291. <https://doi.org/10.1016/j.chemosphere.2015.08.042>.

- 1560 [154] M.W. Yap, N.M. Mubarak, J.N. Sahu, E.C. Abdullah, Microwave induced synthesis
1561 of magnetic biochar from agricultural biomass for removal of lead and cadmium from
1562 wastewater, *J. Ind. Eng. Chem.* 45 (2017) 287–295.
1563 <https://doi.org/10.1016/j.jiec.2016.09.036>.
- 1564 [155] E.B. Son, K.M. Poo, J.S. Chang, K.J. Chae, Heavy metal removal from aqueous
1565 solutions using engineered magnetic biochars derived from waste marine macro-
1566 algal biomass, *Sci. Total Environ.* 615 (2018) 161–168.
1567 <https://doi.org/10.1016/j.scitotenv.2017.09.171>.
- 1568 [156] J. Yang, Y. Zhao, S. Ma, B. Zhu, J. Zhang, C. Zheng, Mercury Removal by Magnetic
1569 Biochar Derived from Simultaneous Activation and Magnetization of Sawdust,
1570 *Environ. Sci. Technol.* 50 (2016) 12040–12047.
1571 <https://doi.org/10.1021/acs.est.6b03743>.
- 1572 [157] K. Vijayaraghavan, The importance of mineral ingredients in biochar production,
1573 properties and applications, *Crit. Rev. Environ. Sci. Technol.* 51 (2021) 113–139.
1574 <https://doi.org/10.1080/10643389.2020.1716654>.
- 1575 [158] X. Yang, Y. Wan, Y. Zheng, F. He, Z. Yu, J. Huang, H. Wang, Y.S. Ok, Y. Jiang, B.
1576 Gao, Surface functional groups of carbon-based adsorbents and their roles in the
1577 removal of heavy metals from aqueous solutions: A critical review, *Chem. Eng. J.*
1578 366 (2019) 608–621. <https://doi.org/10.1016/j.cej.2019.02.119>.
- 1579 [159] X. fei Tan, Y. guo Liu, Y. ling Gu, Y. Xu, G. ming Zeng, X. jiang Hu, S. bo Liu, X.
1580 Wang, S. mian Liu, J. Li, Biochar-based nano-composites for the decontamination
1581 of wastewater: A review, *Bioresour. Technol.* 212 (2016) 318–333.
1582 <https://doi.org/10.1016/j.biortech.2016.04.093>.
- 1583 [160] L. Dai, Q. Lu, H. Zhou, F. Shen, Z. Liu, W. Zhu, H. Huang, Tuning oxygenated
1584 functional groups on biochar for water pollution control: A critical review, *J. Hazard.*
1585 *Mater.* 420 (2021) 126547. <https://doi.org/10.1016/j.jhazmat.2021.126547>.
- 1586 [161] J.J. Wang, R. Li, J.J. Wang, L.A. Gaston, B. Zhou, M. Li, R. Xiao, An overview of
1587 carbothermal synthesis of metal – biochar composites for the removal of oxyanion
1588 contaminants from aqueous solution An overview of carbothermal synthesis of

1589 metal e biochar composites for the removal of oxyanion contaminants from aqueous
1590 so, Carbon N. Y. 129 (2018) 674–687.
1591 <https://doi.org/10.1016/j.carbon.2017.12.070>.

1592 [162] P. Liu, W.J. Liu, H. Jiang, J.J. Chen, W.W. Li, H.Q. Yu, Modification of bio-char
1593 derived from fast pyrolysis of biomass and its application in removal of tetracycline
1594 from aqueous solution, Bioresour. Technol. 121 (2012) 235–240.
1595 <https://doi.org/10.1016/j.biortech.2012.06.085>.

1596 [163] W. Shen, Z. Li, Y. Liu, Surface Chemical Functional Groups Modification of Porous
1597 Carbon, Recent Patents Chem. Eng. 1 (2012) 27–40.
1598 <https://doi.org/10.2174/2211334710801010027>.

1599 [164] M. Ahmaruzzaman, Biochar based nanocomposites for photocatalytic degradation
1600 of emerging organic pollutants from water and wastewater, Mater. Res. Bull. 140
1601 (2021) 111262. <https://doi.org/10.1016/j.materresbull.2021.111262>.

1602 [165] J. Sun, X. Lin, J. Xie, Y. Zhang, Q. Wang, Z. Ying, Facile synthesis of novel ternary
1603 g-C₃N₄/ferrite/biochar hybrid photocatalyst for efficient degradation of methylene
1604 blue under visible-light irradiation, Colloids Surfaces A Physicochem. Eng. Asp. 606
1605 (2020) 125556. <https://doi.org/10.1016/j.colsurfa.2020.125556>.

1606 [166] S.Q. Tian, J.Y. Qi, Y.P. Wang, Y.L. Liu, L. Wang, J. Ma, Heterogeneous catalytic
1607 ozonation of atrazine with Mn-loaded and Fe-loaded biochar, Water Res. 193
1608 (2021) 116860. <https://doi.org/10.1016/j.watres.2021.116860>.

1609 [167] N. Cheng, B. Wang, P. Wu, X. Lee, Y. Xing, M. Chen, B. Gao, Adsorption of
1610 emerging contaminants from water and wastewater by modified biochar: A review,
1611 Environ. Pollut. 273 (2021) 116448. <https://doi.org/10.1016/j.envpol.2021.116448>.

1612 [168] K. Zoroufchi Benis, A. Motalebi Damuchali, J. Soltan, K.N. McPhedran, Treatment
1613 of aqueous arsenic – A review of biochar modification methods, Sci. Total Environ.
1614 739 (2020) 139750. <https://doi.org/10.1016/j.scitotenv.2020.139750>.

1615 [169] Y. Cao, S. Jiang, Y. Zhang, J. Xu, L. Qiu, L. Wang, Investigation into adsorption
1616 characteristics and mechanism of atrazine on nano-MgO modified fallen leaf

- 1617 biochar, J. Environ. Chem. Eng. 9 (2021) 105727.
1618 <https://doi.org/10.1016/j.jece.2021.105727>.
- 1619 [170] R.Z. Wang, D.L. Huang, Y.G. Liu, C. Zhang, C. Lai, X. Wang, G.M. Zeng, Q. Zhang,
1620 X.M. Gong, P. Xu, Synergistic removal of copper and tetracycline from aqueous
1621 solution by steam-activated bamboo-derived biochar, J. Hazard. Mater. 384 (2020)
1622 121470. <https://doi.org/10.1016/j.jhazmat.2019.121470>.
- 1623 [171] D.D. Sewu, H. Jung, S.S. Kim, D.S. Lee, S.H. Woo, Decolorization of cationic and
1624 anionic dye-laden wastewater by steam-activated biochar produced at an industrial-
1625 scale from spent mushroom substrate, Bioresour. Technol. 277 (2019) 77–86.
1626 <https://doi.org/10.1016/j.biortech.2019.01.034>.
- 1627 [172] Y. You, Z. Shi, Y. Li, Z. Zhao, B. He, X. Cheng, Magnetic cobalt ferrite biochar
1628 composite as peroxymonosulfate activator for removal of lomefloxacin
1629 hydrochloride, Sep. Purif. Technol. 272 (2021).
1630 <https://doi.org/10.1016/j.seppur.2021.118889>.
- 1631 [173] L. Chen, X. Jiang, R. Xie, Y. Zhang, Y. Jin, W. Jiang, A novel porous biochar-
1632 supported Fe-Mn composite as a persulfate activator for the removal of acid red 88,
1633 Sep. Purif. Technol. 250 (2020) 117232.
1634 <https://doi.org/10.1016/j.seppur.2020.117232>.
- 1635 [174] K.A. Azalok, A.A. Oladipo, M. Gazi, UV-light-induced photocatalytic performance of
1636 reusable MnFe-LDO–biochar for tetracycline removal in water, J. Photochem.
1637 Photobiol. A Chem. 405 (2021) 112976.
1638 <https://doi.org/10.1016/j.jphotochem.2020.112976>.
- 1639 [175] Y. Xiao, H. Lyu, C. Yang, B. Zhao, L. Wang, J. Tang, Graphitic carbon
1640 nitride/biochar composite synthesized by a facile ball-milling method for the
1641 adsorption and photocatalytic degradation of enrofloxacin, J. Environ. Sci. (China).
1642 103 (2021) 93–107. <https://doi.org/10.1016/j.jes.2020.10.006>.
- 1643 [176] H. Wang, W. Guo, B. Liu, Q. Si, H. Luo, Q. Zhao, N. Ren, Sludge-derived biochar
1644 as efficient persulfate activators: Sulfurization-induced electronic structure
1645 modulation and disparate nonradical mechanisms, Appl. Catal. B Environ. 279

- 1646 (2020) 119361. <https://doi.org/10.1016/j.apcatb.2020.119361>.
- 1647 [177] P. Borthakur, M. Aryafard, Z. Zara, Ā. David, B. Minofar, M.R. Das, M. Vithanage,
1648 Computational and experimental assessment of pH and specific ions on the solute
1649 solvent interactions of clay-biochar composites towards tetracycline adsorption:
1650 Implications on wastewater treatment, *J. Environ. Manage.* 283 (2021).
1651 <https://doi.org/10.1016/j.jenvman.2021.111989>.
- 1652 [178] Y. Ma, P. Li, L. Yang, L. Wu, L. He, F. Gao, X. Qi, Z. Zhang, Iron/zinc and phosphoric
1653 acid modified sludge biochar as an efficient adsorbent for fluoroquinolones
1654 antibiotics removal, *Ecotoxicol. Environ. Saf.* 196 (2020).
1655 <https://doi.org/10.1016/j.ecoenv.2020.110550>.
- 1656 [179] Y. Zheng, Y. Wan, J. Chen, H. Chen, B. Gao, MgO modified biochar produced
1657 through ball milling: A dual-functional adsorbent for removal of different
1658 contaminants, *Chemosphere.* 243 (2020) 125344.
1659 <https://doi.org/10.1016/j.chemosphere.2019.125344>.
- 1660 [180] Q. Zhang, J. Wang, H. Lyu, Q. Zhao, L. Jiang, L. Liu, Ball-milled biochar for
1661 galaxolide removal: Sorption performance and governing mechanisms, *Sci. Total*
1662 *Environ.* 659 (2019) 1537–1545. <https://doi.org/10.1016/j.scitotenv.2019.01.005>.
- 1663 [181] C.E.R. Barquilha, M.C.B. Braga, Adsorption of organic and inorganic pollutants onto
1664 biochars: Challenges, operating conditions, and mechanisms, *Bioresour. Technol.*
1665 *Reports.* 15 (2021) 100728. <https://doi.org/10.1016/j.biteb.2021.100728>.
- 1666 [182] A. Gopinath, G. Divyapriya, V. Srivastava, A.R. Laiju, P. V. Nidheesh, M.S. Kumar,
1667 Conversion of sewage sludge into biochar: A potential resource in water and
1668 wastewater treatment, *Environ. Res.* 194 (2021) 110656.
1669 <https://doi.org/10.1016/j.envres.2020.110656>.
- 1670 [183] H. Dong, C. Zhang, J. Deng, Z. Jiang, L. Zhang, Y. Cheng, K. Hou, L. Tang, G.
1671 Zeng, Factors influencing degradation of trichloroethylene by sulfide-modified
1672 nanoscale zero-valent iron in aqueous solution, *Water Res.* 135 (2018) 1–10.
1673 <https://doi.org/10.1016/j.watres.2018.02.017>.

- 1674 [184] X. Yang, G. Xu, H. Yu, Z. Zhang, Preparation of ferric-activated sludge-based
1675 adsorbent from biological sludge for tetracycline removal, *Bioresour. Technol.* 211
1676 (2016) 566–573. <https://doi.org/10.1016/j.biortech.2016.03.140>.
- 1677 [185] C.M. Navarathna, N. Bombuwala Dewage, C. Keeton, J. Pennisson, R. Henderson,
1678 B. Lashley, X. Zhang, E.B. Hassan, F. Perez, D. Mohan, C.U. Pittman, T. Mlsna,
1679 Biochar Adsorbents with Enhanced Hydrophobicity for Oil Spill Removal, *ACS Appl.*
1680 *Mater. Interfaces.* 12 (2020) 9248–9260. <https://doi.org/10.1021/acsami.9b20924>.
- 1681 [186] N. Zulbadli, N. Zaini, L.Y. Soon, T.Y. Kang, A.A.A. Al-Harf, N.S. Nasri, K.S.N.
1682 Kamarudin, Acid-modified adsorbents from sustainable green-based materials for
1683 crude oil removal, *J. Adv. Res. Fluid Mech. Therm. Sci.* 46 (2018) 11–20.
- 1684 [187] S.A. Osemeahon, B.J. Dimas, Removal of Crude Oil from Aqueous Medium by
1685 Sorption on *Sterculis setigera*, *Asian J. Appl. Chem. Res.* 10 (2020) 1–12.
1686 <https://doi.org/10.9734/ajacr/2020/v5i330133>.
- 1687 [188] R. Gurav, S.K. Bhatia, T.R. Choi, Y.K. Choi, H.J. Kim, H.S. Song, S.L. Park, H.S.
1688 Lee, S.M. Lee, K.Y. Choi, Y.H. Yang, Adsorptive removal of crude petroleum oil
1689 from water using floating pinewood biochar decorated with coconut oil-derived fatty
1690 acids, *Sci. Total Environ.* 781 (2021) 146636.
1691 <https://doi.org/10.1016/j.scitotenv.2021.146636>.
- 1692 [189] H.H. Cho, K. Wepasnick, B.A. Smith, F.K. Bangash, D.H. Fairbrother, W.P. Ball,
1693 Sorption of aqueous Zn[II] and Cd[II] by multiwall carbon nanotubes: The relative
1694 roles of oxygen-containing functional groups and graphenic carbon, *Langmuir.* 26
1695 (2010) 967–981. <https://doi.org/10.1021/la902440u>.
- 1696 [190] Y. Zheng, J. Wang, D. Li, C. Liu, Y. Lu, X. Lin, Z. Zheng, Insight into the
1697 KOH/KMnO₄ activation mechanism of oxygen-enriched hierarchical porous biochar
1698 derived from biomass waste by in-situ pyrolysis for methylene blue enhanced
1699 adsorption, *J. Anal. Appl. Pyrolysis.* 158 (2021) 105269.
1700 <https://doi.org/10.1016/j.jaap.2021.105269>.
- 1701 [191] A.S.I. Abdoul Magid, M.S. Islam, Y. Chen, L. Weng, J. Li, J. Ma, Y. Li, Enhanced
1702 adsorption of polystyrene nanoplastics (PSNPs) onto oxidized corncob biochar with

- 1703 high pyrolysis temperature, *Sci. Total Environ.* 784 (2021).
1704 <https://doi.org/10.1016/j.scitotenv.2021.147115>.
- 1705 [192] B.M. Córdova, J.P. Santa Cruz, T.V.M. Ocampo, R.G. Huamani-Palomino, A.M.
1706 Baena-Moncada, Simultaneous adsorption of a ternary mixture of brilliant green,
1707 rhodamine B and methyl orange as artificial wastewater onto biochar from cocoa
1708 pod husk waste. Quantification of dyes using the derivative spectrophotometry
1709 method, *New J. Chem.* 44 (2020) 8303–8316. <https://doi.org/10.1039/d0nj00916d>.
- 1710 [193] J. Shin, J. Kwak, Y.G. Lee, S. Kim, M. Choi, S. Bae, S.H. Lee, Y. Park, K. Chon,
1711 Competitive adsorption of pharmaceuticals in lake water and wastewater effluent by
1712 pristine and NaOH-activated biochars from spent coffee wastes: Contribution of
1713 hydrophobic and π - π interactions, *Environ. Pollut.* 270 (2021) 116244.
1714 <https://doi.org/10.1016/j.envpol.2020.116244>.
- 1715 [194] R.V. Piloni, L. Fontes Coelho, D.C. Sass, M. Lanteri, M.A. Zaghete Bertochi, E.
1716 Laura Moyano, J. Contiero, Biochars from Spirulina as an alternative material in the
1717 purification of lactic acid from a fermentation broth, *Curr. Res. Green Sustain.*
1718 *Chem.* 4 (2021). <https://doi.org/10.1016/j.crgsc.2021.100084>.
- 1719 [195] R. Tian, H. Dong, J. Chen, R. Li, Q. Xie, Amorphous Co₃O₄ nanoparticles-
1720 decorated biochar as an efficient activator of peroxydisulfate for the removal of
1721 sulfamethazine in aqueous solution, *Sep. Purif. Technol.* 250 (2020) 117246.
1722 <https://doi.org/10.1016/j.seppur.2020.117246>.
- 1723 [196] Y. Zhao, X. Yuan, X. Li, L. Jiang, H. Wang, Burgeoning prospects of biochar and its
1724 composite in persulfate-advanced oxidation process, *J. Hazard. Mater.* 409 (2021)
1725 124893. <https://doi.org/10.1016/j.jhazmat.2020.124893>.
- 1726 [197] J. Chen, X. Yu, C. Li, X. Tang, Y. Sun, Removal of tetracycline via the synergistic
1727 effect of biochar adsorption and enhanced activation of persulfate, *Chem. Eng. J.*
1728 382 (2020) 122916. <https://doi.org/10.1016/j.cej.2019.122916>.
- 1729 [198] J. Wang, S. Wang, Activation of persulfate (PS) and peroxydisulfate (PMS) and
1730 application for the degradation of emerging contaminants, *Chem. Eng. J.* 334 (2018)
1731 1502–1517. <https://doi.org/10.1016/j.cej.2017.11.059>.

- 1732 [199] X. Fan, H. Lin, J. Zhao, Y. Mao, J. Zhang, H. Zhang, Activation of
1733 peroxymonosulfate by sewage sludge biochar-based catalyst for efficient removal
1734 of bisphenol A: Performance and mechanism, *Sep. Purif. Technol.* 272 (2021)
1735 118909. <https://doi.org/10.1016/j.seppur.2021.118909>.
- 1736 [200] N. Hagemann, K. Spokas, H.P. Schmidt, R. Kägi, M.A. Böhler, T.D. Bucheli,
1737 Activated carbon, biochar and charcoal: Linkages and synergies across pyrogenic
1738 carbon's ABCs, *Water* (Switzerland). 10 (2018) 1–19.
1739 <https://doi.org/10.3390/w10020182>.
- 1740 [201] A. Méndez, G. Gascó, M.M.A. Freitas, G. Siebielec, T. Stuczynski, J.L. Figueiredo,
1741 Preparation of carbon-based adsorbents from pyrolysis and air activation of sewage
1742 sludges, *Chem. Eng. J.* 108 (2005) 169–177.
1743 <https://doi.org/10.1016/j.cej.2005.01.015>.
- 1744 [202] I. Ibrahim, M.A. Hassan, S. Abd-Aziz, Y. Shirai, Y. Andou, M.R. Othman, A.A.M. Ali,
1745 M.R. Zakaria, Reduction of residual pollutants from biologically treated palm oil mill
1746 effluent final discharge by steam activated bioadsorbent from oil palm biomass, *J.*
1747 *Clean. Prod.* 141 (2017) 122–127. <https://doi.org/10.1016/j.jclepro.2016.09.066>.
- 1748 [203] Q. Jia, A.C. Lua, Effects of pyrolysis conditions on the physical characteristics of oil-
1749 palm-shell activated carbons used in aqueous phase phenol adsorption, *J. Anal.*
1750 *Appl. Pyrolysis.* 83 (2008) 175–179. <https://doi.org/10.1016/j.jaap.2008.08.001>.
- 1751 [204] H. Jin, S. Capareda, Z. Chang, J. Gao, Y. Xu, J. Zhang, Biochar pyrolytically
1752 produced from municipal solid wastes for aqueous As(V) removal: Adsorption
1753 property and its improvement with KOH activation, *Bioresour. Technol.* 169 (2014)
1754 622–629. <https://doi.org/10.1016/j.biortech.2014.06.103>.
- 1755 [205] M. Arif, G. Liu, B. Yousaf, R. Ahmed, S. Irshad, A. Ashraf, M. Zia-ur-Rehman, M.S.
1756 Rashid, Synthesis, characteristics and mechanistic insight into the clays and clay
1757 minerals-biochar surface interactions for contaminants removal-A review, *J. Clean.*
1758 *Prod.* 310 (2021) 127548. <https://doi.org/10.1016/j.jclepro.2021.127548>.
- 1759 [206] B. Wang, B. Gao, J. Fang, Recent advances in engineered biochar productions and
1760 applications, *Crit. Rev. Environ. Sci. Technol.* 47 (2017) 2158–2207.

- 1761 <https://doi.org/10.1080/10643389.2017.1418580>.
- 1762 [207] S.C. Peterson, M.A. Jackson, S. Kim, D.E. Palmquist, Increasing biochar surface
1763 area: Optimization of ball milling parameters, *Powder Technol.* 228 (2012) 115–120.
1764 <https://doi.org/10.1016/j.powtec.2012.05.005>.
- 1765 [208] H. Lyu, B. Gao, F. He, A.R. Zimmerman, C. Ding, H. Huang, J. Tang, Effects of ball
1766 milling on the physicochemical and sorptive properties of biochar: Experimental
1767 observations and governing mechanisms, *Environ. Pollut.* 233 (2018) 54–63.
1768 <https://doi.org/10.1016/j.envpol.2017.10.037>.
- 1769 [209] D.D. Sewu, H.N. Tran, G. Ohemeng-Boahen, S.H. Woo, Facile magnetic biochar
1770 production route with new goethite nanoparticle precursor, *Sci. Total Environ.* 717
1771 (2020) 137091. <https://doi.org/10.1016/j.scitotenv.2020.137091>.
- 1772 [210] X. Li, C. Wang, J. Zhang, J. Liu, B. Liu, G. Chen, Preparation and application of
1773 magnetic biochar in water treatment: A critical review, *Sci. Total Environ.* 711 (2020)
1774 134847. <https://doi.org/10.1016/j.scitotenv.2019.134847>.
- 1775 [211] Z. Feng, R. Yuan, F. Wang, Z. Chen, B. Zhou, H. Chen, Preparation of magnetic
1776 biochar and its application in catalytic degradation of organic pollutants: A review,
1777 *Sci. Total Environ.* 765 (2021) 142673.
1778 <https://doi.org/10.1016/j.scitotenv.2020.142673>.
- 1779 [212] D. Harikishore Kumar Reddy, S.M. Lee, Magnetic biochar composite: Facile
1780 synthesis, characterization, and application for heavy metal removal, *Colloids
1781 Surfaces A Physicochem. Eng. Asp.* 454 (2014) 96–103.
1782 <https://doi.org/10.1016/j.colsurfa.2014.03.105>.
- 1783 [213] S. Qu, F. Huang, S. Yu, G. Chen, J. Kong, Magnetic removal of dyes from aqueous
1784 solution using multi-walled carbon nanotubes filled with Fe₂O₃ particles, *J. Hazard.
1785 Mater.* 160 (2008) 643–647. <https://doi.org/10.1016/j.jhazmat.2008.03.037>.
- 1786 [214] K.R. Thines, E.C. Abdullah, N.M. Mubarak, M. Ruthiraan, Synthesis of magnetic
1787 biochar from agricultural waste biomass to enhancing route for waste water and
1788 polymer application: A review, *Renew. Sustain. Energy Rev.* 67 (2017) 257–276.

- 1789 <https://doi.org/10.1016/j.rser.2016.09.057>.
- 1790 [215] S.K. Theydan, M.J. Ahmed, Adsorption of methylene blue onto biomass-based
1791 activated carbon by FeCl₃ activation: Equilibrium, kinetics, and thermodynamic
1792 studies, *J. Anal. Appl. Pyrolysis*. 97 (2012) 116–122.
1793 <https://doi.org/10.1016/j.jaap.2012.05.008>.
- 1794 [216] M. Ruthiraan, N.M. Mubarak, R.K. Thines, E.C. Abdullah, J.N. Sahu, N.S.
1795 Jayakumar, P. Ganesan, Comparative kinetic study of functionalized carbon
1796 nanotubes and magnetic biochar for removal of Cd²⁺ ions from wastewater, *Korean
1797 J. Chem. Eng.* 32 (2015) 446–457. <https://doi.org/10.1007/s11814-014-0260-7>.
- 1798 [217] S. Wang, B. Gao, A.R. Zimmerman, Y. Li, L. Ma, W.G. Harris, K.W. Migliaccio,
1799 Removal of arsenic by magnetic biochar prepared from pinewood and natural
1800 hematite, *Bioresour. Technol.* 175 (2015) 391–395.
1801 <https://doi.org/10.1016/j.biortech.2014.10.104>.
- 1802 [218] S.A. Baig, J. Zhu, N. Muhammad, T. Sheng, X. Xu, Effect of synthesis methods on
1803 magnetic Kans grass biochar for enhanced As(III, V) adsorption from aqueous
1804 solutions, *Biomass and Bioenergy*. 71 (2014) 299–310.
1805 <https://doi.org/10.1016/j.biombioe.2014.09.027>.
- 1806 [219] B. Chen, Z. Chen, S. Lv, A novel magnetic biochar efficiently sorbs organic
1807 pollutants and phosphate, *Bioresour. Technol.* 102 (2011) 716–723.
1808 <https://doi.org/10.1016/j.biortech.2010.08.067>.
- 1809 [220] Y. Han, X. Cao, X. Ouyang, S.P. Sohi, J. Chen, Adsorption kinetics of magnetic
1810 biochar derived from peanut hull on removal of Cr (VI) from aqueous solution:
1811 Effects of production conditions and particle size, *Chemosphere*. 145 (2016) 336–
1812 341. <https://doi.org/10.1016/j.chemosphere.2015.11.050>.
- 1813 [221] S.Q. Chen, Y.L. Chen, H. Jiang, Slow Pyrolysis Magnetization of Hydrochar for
1814 Effective and Highly Stable Removal of Tetracycline from Aqueous Solution, *Ind.
1815 Eng. Chem. Res.* 56 (2017) 3059–3066. <https://doi.org/10.1021/acs.iecr.6b04683>.
- 1816 [222] M. Zhang, B. Gao, S. Varnoosfaderani, A. Hebard, Y. Yao, M. Inyang, Preparation

- 1817 and characterization of a novel magnetic biochar for arsenic removal, *Bioresour.*
1818 *Technol.* 130 (2013) 457–462. <https://doi.org/10.1016/j.biortech.2012.11.132>.
- 1819 [223] X. Zhu, Y. Liu, G. Luo, F. Qian, S. Zhang, J. Chen, Facile fabrication of magnetic
1820 carbon composites from hydrochar via simultaneous activation and magnetization
1821 for triclosan adsorption, *Environ. Sci. Technol.* 48 (2014) 5840–5848.
1822 <https://doi.org/10.1021/es500531c>.
- 1823 [224] J. Zhao, G. Liang, X. Zhang, X. Cai, R. Li, X. Xie, Z. Wang, Coating magnetic biochar
1824 with humic acid for high efficient removal of fluoroquinolone antibiotics in water, *Sci.*
1825 *Total Environ.* 688 (2019) 1205–1215.
1826 <https://doi.org/10.1016/j.scitotenv.2019.06.287>.
- 1827 [225] X. Wang, J. Xu, J. Liu, J. Liu, F. Xia, C. Wang, R.A. Dahlgren, W. Liu, Mechanism
1828 of Cr(VI) removal by magnetic greigite/biochar composites, *Sci. Total Environ.* 700
1829 (2020) 134414. <https://doi.org/10.1016/j.scitotenv.2019.134414>.
- 1830 [226] G. Zhang, J. Qu, H. Liu, A.T. Cooper, R. Wu, CuFe₂O₄/activated carbon composite:
1831 A novel magnetic adsorbent for the removal of acid orange II and catalytic
1832 regeneration, *Chemosphere.* 68 (2007) 1058–1066.
1833 <https://doi.org/10.1016/j.chemosphere.2007.01.081>.
- 1834 [227] S. Wang, B. Gao, Y. Li, Y. Wan, A.E. Creamer, Sorption of arsenate onto magnetic
1835 iron-manganese (Fe-Mn) biochar composites, *RSC Adv.* 5 (2015) 67971–67978.
1836 <https://doi.org/10.1039/c5ra12137j>.
- 1837 [228] C. Fang, T. Zhang, P. Li, R. Jiang, S. Wu, H. Nie, Y. Wang, Phosphorus recovery
1838 from biogas fermentation liquid by Ca-Mg loaded biochar, *J. Environ. Sci. (China).*
1839 29 (2015) 106–114. <https://doi.org/10.1016/j.jes.2014.08.019>.
- 1840 [229] J.X. Yu, L.Y. Wang, R.A. Chi, Y.F. Zhang, Z.G. Xu, J. Guo, Competitive adsorption
1841 of Pb²⁺ and Cd²⁺ on magnetic modified sugarcane bagasse prepared by two
1842 simple steps, *Appl. Surf. Sci.* 268 (2013) 163–170.
1843 <https://doi.org/10.1016/j.apsusc.2012.12.047>.
- 1844 [230] L. Lian, X. Cao, Y. Wu, D. Sun, D. Lou, A green synthesis of magnetic bentonite

- 1845 material and its application for removal of microcystin-LR in water, *Appl. Surf. Sci.*
1846 289 (2014) 245–251. <https://doi.org/10.1016/j.apsusc.2013.10.144>.
- 1847 [231] L. Peng, Y. Ren, J. Gu, P. Qin, Q. Zeng, J. Shao, M. Lei, L. Chai, Iron improving
1848 bio-char derived from microalgae on removal of tetracycline from aqueous system,
1849 *Environ. Sci. Pollut. Res.* 21 (2014) 7631–7640. [https://doi.org/10.1007/s11356-](https://doi.org/10.1007/s11356-014-2677-2)
1850 014-2677-2.
- 1851 [232] N. Cheng, B. Wang, P. Wu, X. Lee, Y. Xing, M. Chen, B. Gao, Adsorption of
1852 emerging contaminants from water and wastewater by modified biochar: A review,
1853 *Environ. Pollut.* 273 (2021) 116448. <https://doi.org/10.1016/j.envpol.2021.116448>.
- 1854 [233] C. Fu, H. Zhang, M. Xia, W. Lei, F. Wang, The single/co-adsorption characteristics
1855 and microscopic adsorption mechanism of biochar-montmorillonite composite
1856 adsorbent for pharmaceutical emerging organic contaminant atenolol and lead ions,
1857 *Ecotoxicol. Environ. Saf.* 187 (2020) 109763.
1858 <https://doi.org/10.1016/j.ecoenv.2019.109763>.
- 1859 [234] K.S.D. Premarathna, A.U. Rajapaksha, N. Adassoriya, B. Sarkar, N.M.S. Sirimuthu,
1860 A. Cooray, Y.S. Ok, M. Vithanage, Clay-biochar composites for sorptive removal of
1861 tetracycline antibiotic in aqueous media, *J. Environ. Manage.* 238 (2019) 315–322.
1862 <https://doi.org/10.1016/j.jenvman.2019.02.069>.
- 1863 [235] Z. Zhao, W. Zhou, Insight into interaction between biochar and soil minerals in
1864 changing biochar properties and adsorption capacities for sulfamethoxazole,
1865 *Environ. Pollut.* 245 (2019) 208–217. <https://doi.org/10.1016/j.envpol.2018.11.013>.
- 1866 [236] J. Lu, Y. Yang, P. Liu, Y. Li, F. Huang, L. Zeng, Y. Liang, S. Li, B. Hou, Iron-
1867 montmorillonite treated corn straw biochar: Interfacial chemical behavior and
1868 stability, *Sci. Total Environ.* 708 (2020) 134773.
1869 <https://doi.org/10.1016/j.scitotenv.2019.134773>.
- 1870 [237] H. Han, M.K. Rafiq, T. Zhou, R. Xu, O. Mašek, X. Li, A critical review of clay-based
1871 composites with enhanced adsorption performance for metal and organic pollutants,
1872 *J. Hazard. Mater.* 369 (2019) 780–796.
1873 <https://doi.org/10.1016/j.jhazmat.2019.02.003>.

- 1874 [238] D.D. Sewu, S.H. Woo, D.S. Lee, Biochar from the co-pyrolysis of Saccharina
1875 japonica and goethite as an adsorbent for basic blue 41 removal from aqueous
1876 solution, *Sci. Total Environ.* 797 (2021) 149160.
1877 <https://doi.org/10.1016/j.scitotenv.2021.149160>.
- 1878 [239] N. Liu, C. Wu, G. Lyu, M. Li, Efficient adsorptive removal of short-chain
1879 perfluoroalkyl acids using reed straw-derived biochar (RESCA), *Sci. Total Environ.*
1880 798 (2021) 149191. <https://doi.org/10.1016/j.scitotenv.2021.149191>.
- 1881 [240] Z. Liu, D. Tian, F. Shen, L. Long, Y. Zhang, G. Yang, Y. Zeng, J. Zhang, J. He, Y.
1882 Zhu, S. Deng, Elucidating dominant factors of PO₄³⁻, Cd²⁺ and nitrobenzene
1883 removal by biochar: A comparative investigation based on distinguishable biochars,
1884 *Chinese Chem. Lett.* 30 (2019) 2221–2224.
1885 <https://doi.org/10.1016/j.ccllet.2019.04.016>.
- 1886 [241] M. Wiśniewska, P. Nowicki, K. Szewczuk-Karpisz, M. Gęca, K. Jędruchiewicz, P.
1887 Oleszczuk, Simultaneous removal of toxic Pb(II) ions, poly(acrylic acid) and Triton
1888 X-100 from their mixed solution using engineered biochars obtained from horsetail
1889 herb precursor – Impact of post-activation treatment, *Sep. Purif. Technol.* 276
1890 (2021). <https://doi.org/10.1016/j.seppur.2021.119297>.
- 1891 [242] Z. Wang, M. Sedighi, A. Lea-Langton, Filtration of microplastic spheres by biochar:
1892 removal efficiency and immobilisation mechanisms, *Water Res.* 184 (2020) 116165.
1893 <https://doi.org/10.1016/j.watres.2020.116165>.
- 1894 [243] S. Werner, K. Kätzl, M. Wichern, A. Buerkert, C. Steiner, B. Marschner, Agronomic
1895 benefits of biochar as a soil amendment after its use as waste water filtration
1896 medium, *Environ. Pollut.* 233 (2018) 561–568.
1897 <https://doi.org/10.1016/j.envpol.2017.10.048>.
- 1898 [244] K. Kaetzl, M. Lübken, E. Nettmann, S. Krimmler, M. Wichern, Slow sand filtration of
1899 raw wastewater using biochar as an alternative filtration media, *Sci. Rep.* 10 (2020)
1900 1–11. <https://doi.org/10.1038/s41598-020-57981-0>.
- 1901 [245] K.R. Reddy, T. Xie, S. Dastgheibi, Evaluation of Biochar as a Potential Filter Media
1902 for the Removal of Mixed Contaminants from Urban Storm Water Runoff, *J. Environ.*

- 1903 Eng. 140 (2014) 04014043. [https://doi.org/10.1061/\(asce\)ee.1943-7870.0000872](https://doi.org/10.1061/(asce)ee.1943-7870.0000872).
- 1904 [246] C. Wang, R. Huang, R. Sun, J. Yang, M. Sillanpää, A review on persulfates
1905 activation by functional biochar for organic contaminants removal: Synthesis,
1906 characterizations, radical determination, and mechanism, *J. Environ. Chem. Eng.* 9
1907 (2021) 106267. <https://doi.org/10.1016/j.jece.2021.106267>.
- 1908 [247] Faheem, J. Du, S.H. Kim, M.A. Hassan, S. Irshad, J. Bao, Application of biochar in
1909 advanced oxidation processes: supportive, adsorptive, and catalytic role, *Environ.*
1910 *Sci. Pollut. Res.* 27 (2020) 37286–37312. [https://doi.org/10.1007/s11356-020-](https://doi.org/10.1007/s11356-020-07612-y)
1911 [07612-y](https://doi.org/10.1007/s11356-020-07612-y).
- 1912 [248] D. Huang, Y. Wang, C. Zhang, G. Zeng, C. Lai, J. Wan, L. Qin, Y. Zeng, Influence
1913 of morphological and chemical features of biochar on hydrogen peroxide activation:
1914 Implications on sulfamethazine degradation, *RSC Adv.* 6 (2016) 73186–73196.
1915 <https://doi.org/10.1039/c6ra11850j>.
- 1916 [249] X. Pan, Z. Gu, W. Chen, Q. Li, Preparation of biochar and biochar composites and
1917 their application in a Fenton-like process for wastewater decontamination: A review,
1918 *Sci. Total Environ.* 754 (2021) 142104.
1919 <https://doi.org/10.1016/j.scitotenv.2020.142104>.
- 1920 [250] A. Kumar, K. Saini, T. Bhaskar, Advances in design strategies for preparation of
1921 biochar based catalytic system for production of high value chemicals, *Bioresour.*
1922 *Technol.* 299 (2020) 122564. <https://doi.org/10.1016/j.biortech.2019.122564>.
- 1923 [251] P. V. Nidheesh, A. Gopinath, N. Ranjith, A. Praveen Akre, V. Sreedharan, M. Suresh
1924 Kumar, Potential role of biochar in advanced oxidation processes: A sustainable
1925 approach, *Chem. Eng. J.* 405 (2021) 126582.
1926 <https://doi.org/10.1016/j.cej.2020.126582>.
- 1927 [252] J. Leichtweis, S. Silvestri, E. Carissimi, New composite of pecan nutshells biochar-
1928 ZnO for sequential removal of acid red 97 by adsorption and photocatalysis,
1929 *Biomass and Bioenergy.* 140 (2020) 105648.
1930 <https://doi.org/10.1016/j.biombioe.2020.105648>.

- 1931 [253] L. He, Z. Liu, J. Hu, C. Qin, L. Yao, Y. Zhang, Y. Piao, Sugarcane biochar as novel
 1932 catalyst for highly efficient oxidative removal of organic compounds in water, *Chem.*
 1933 *Eng. J.* 405 (2021) 126895. <https://doi.org/10.1016/j.cej.2020.126895>.
- 1934 [254] J. Lou, Y. Wei, M. Zhang, Q. Meng, J. An, M. Jia, Removal of tetracycline
 1935 hydrochloride in aqueous by coupling dielectric barrier discharge plasma with
 1936 biochar, *Sep. Purif. Technol.* 266 (2021) 118515.
 1937 <https://doi.org/10.1016/j.seppur.2021.118515>.
- 1938 [255] A. Kakade, E.S. Salama, H. Han, Y. Zheng, S. Kulshrestha, M. Jalalah, F.A. Harraz,
 1939 S.A. Alsareii, X. Li, World eutrophic pollution of lake and river: Biotreatment potential
 1940 and future perspectives, *Environ. Technol. Innov.* 23 (2021) 101604.
 1941 <https://doi.org/10.1016/j.eti.2021.101604>.
- 1942 [256] N. Ashoori, M. Teixido, S. Spahr, G.H. LeFevre, D.L. Sedlak, R.G. Luthy, Evaluation
 1943 of pilot-scale biochar-amended woodchip bioreactors to remove nitrate, metals, and
 1944 trace organic contaminants from urban stormwater runoff, *Water Res.* 154 (2019)
 1945 1–11. <https://doi.org/10.1016/j.watres.2019.01.040>.
- 1946 [257] D. Park, Y.S. Yun, J.M. Park, The past, present, and future trends of biosorption,
 1947 *Biotechnol. Bioprocess Eng.* 15 (2010) 86–102. <https://doi.org/10.1007/s12257-009-0199-4>.
- 1949 [258] D. Lakshmi, D. Akhil, A. Kartik, K.P. Gopinath, J. Arun, A. Bhatnagar, J. Rinklebe,
 1950 W. Kim, G. Muthusamy, Artificial intelligence (AI) applications in adsorption of heavy
 1951 metals using modified biochar, *Sci. Total Environ.* 801 (2021).
 1952 <https://doi.org/10.1016/j.scitotenv.2021.149623>.
- 1953 [259] S.K. Bhagat, T.M. Tung, Z.M. Yaseen, Development of artificial intelligence for
 1954 modeling wastewater heavy metal removal: State of the art, application assessment
 1955 and possible future research, *J. Clean. Prod.* 250 (2020) 119473.
 1956 <https://doi.org/10.1016/j.jclepro.2019.119473>.
- 1957 [260] X. Zhu, Y. Li, X. Wang, Machine learning prediction of biochar yield and carbon
 1958 contents in biochar based on biomass characteristics and pyrolysis conditions,
 1959 *Bioresour. Technol.* 288 (2019) 121527.

1960 <https://doi.org/10.1016/j.biortech.2019.121527>.

1961 [261] X. Zhu, M. He, Y. Sun, Z. Xu, Z. Wan, D. Hou, D.S. Alessi, D.C.W. Tsang, Insights
1962 into the adsorption of pharmaceuticals and personal care products (PPCPs) on
1963 biochar and activated carbon with the aid of machine learning, J. Hazard. Mater.
1964 423 (2022) 127060. <https://doi.org/10.1016/j.jhazmat.2021.127060>.

1965

Pre-proof